12

A089899

(6) Ocean Tides, Part II:
A Hydrodynamical Interpolation Model,

(10) Ernst W. Schwiderski
U.S. Naval Surface Weapons Center
Dahlgren, Virginia

(11) 1980

(12) 36

The strictly mathematical ocean tide model developed in Part I of this paper is modified in order to include realistic hydrodynamical barrier effects of narrow ocean ridges and other large bottom irregularities. This modification begins with a hydrodynamical redefinition of the ocean bathymetry at over 3,000 grid points, increasing simultaneously the depth data range to: 10m → 7,000m. In a second step a unique hydrodynamical interpolation technique is developed that incorporates into the model over 2,000 empirical tide data collected around the world at continental and island stations. This interpolation is accomplished by a controlled cell-wise adjustment of the bottom friction coefficient and by allowing a monitored in- or out-flow across the mathematical ocean boundary and so, redefining a more physical shoreline. Extensive computer experiments were conducted to study the characteristics of the novel friction laws and hydrodynamical interpolation methods. The computed M_2-tide data along with all (specially labeled) empirical constants are tabulated in map form for four typical 30° by 50° ocean areas. It is estimated that the tabulated tidal charts permit a prediction of the M_2-tide elevation of the ocean surface over the geoidal level with an accuracy of better than 5 cm anywhere

Marine Geodesy, Volume 3
0149-0419/80/0131-0219 $02.00/0

JOB

411567 80 9 26 019

in the open ocean and with somewhat less accuracy near rough shorelines. With the forthcoming construction of the lesser S_2, N_2, and K_2; K_1, O_1, P_1, and Q_1; and Mf, Mm, and Ssa tidal constituents, the total tide-prediction error can be kept below the 10-cm bound posed by applied researchers of today.

In Part I of this paper (Schwiderski, 1979) a purely hydrodynamical ocean tide model has been developed and tested. This model has been applied to compute a preliminary M_2 ocean tidal chart (Schwiderski, 1976, I). (References listed in Part I are indicated by the added, I, after the year specification.) The results were found encouraging and satisfactory for some applications. However, significant shortcomings still persisted, especially over narrow ocean ridges. The remaining deficiencies were attributed to local distortions and retardations of the tidal waves due to hydrodynamical barrier effects of ocean ridges and other bottom irregularities.

In the following Part II of the paper, an attempt will be made to eliminate the shortcomings of the purely theoretical model by using a hydrodynamically defined bathymetry of the oceans and by incorporating directly empirically known tide data into the discrete tide model described in Part I. The latter modification will be accomplished by a controlled local adjustment of the bottom friction coefficient and by allowing a monitored in- or out-flow across the mathematical ocean boundary, and thus redefining implicitly a more physical shoreline. A detailed discussion of the quality of the new M_2 ocean tidal charts will be given in the sections, "Quality of the Ocean-Tide Model" and "Conclusions."

The complete M_2 ocean tide is published in tabulated map form in Schwiderski (1979c I). Similar charts for the S_2, N_2, K_2, O_1, P_1, Q_1, Mf, Mm, and Ssa ocean tides (see Part I, Table 1) are under construction and will be published in additional papers. A separate tabulation of the new hydrodynamically defined ocean bathymetry may be found in Schwiderski (1978a I). All tidal and bathymetry data will be available in tape form at the Naval Surface Weapons Center, Dahlgren, Virginia 22448.

Hydrodynamically Defined Ocean Bathymetry

A reinspection of the bathymetric data revealed clearly that even a 1° by 1° grid scheme falls far short in representing a narrow ocean ridge in a hydrodynamically proper fashion. The defect is particularly compounded when the narrow ridge parallels a deep trench. The reason for this deficiency is obviously the purely hydrostatic character of the averaging principles employed by Smith *et al.* (1966 I) in order to assign a depth value at the center of a mesh cell that is supposed to be representative for the entire cell. For instance, if the area of a mesh cell is (by subjective sight) more than half land, then it is called a "land cell," and the cell is given (for the present purpose) the depth value "zero." In the alternative case, the cell is declared "oceanic," and a depth value is assigned that conserves the estimated actual water mass. Because of those hydrostatic principles, cells were found that contained elongated islands crossing even several cells, but every cell was declared oceanic. Moreover, an oceanic trench portion of the cell with some 7,000-m true depth produced an average depth of more than 3,500 m. Clearly, for ocean current models the entire cell represents an impassable wall, and the depth value should be "zero" instead of 3,500 m.

In order to eliminate the shortcomings of the bathymetric data compiled by Smith *et al.* (1966 I), the depth values were revised by using the following "hydrodynamical" principles:

(a) Boundary cells at or near continental shorelines consisting of more than half oceanic areas of depths larger than 5 m were designated ocean cells, and the average oceanic depth values were assigned as the "hydrodynamically" averaged depths to the entire cells. The new depth value is preferable to the "hydrostatically" averaged depth, which preserves the actual water mass but ascribes artificially a shallow shelf character to the cell.

(b) Island cells were declared terrestrial cells with depths zero if either the island areas were larger than half the mesh areas or the (elongated) island lengths exceeded the mesh diameters.

(c) Island cells that remained oceanic cells were assigned depth values less than the hydrostatically averaged values. In this case and in situations of submerged seamounts or narrow ocean ridges (e.g., Aleutian, Marianas, and Caribbean), the hydrodynamical depths depended on the assessed "barrier" effects of the obstacles: the longer and/or higher the barrier, the lesser the depth. In general, the average "ridge depth" was assigned to the entire cell.

(d) The assigned minimum depth (Part I, Equation 50) was lowered to

$$H_m = \min H(\lambda,\theta) = 20 \text{ m}, \qquad (1)$$

which is further lowered to 10 m by the averaging Equations 65 in Part I. (All notations of Part I are used unchanged in the present paper.)

The hydrodynamically justified principles (a) to (c) are, naturally, quite subjective and by no means free of any error. Nevertheless, some computational experiments indicated only very minor effects of isolated depth data changes. More than 3,000 depth values were changed, but only very few of those required additional readjustments in order to keep some limitation on the first and second derivatives of $H(\lambda,\theta)$; i.e., on the relative differences given by Equation 65 in Part I. Furthermore, the hydrodynamical interpolation of empirical tidal data (section, "Hydrodynamical Interpolation of Empirical Tide Data") known at continental and island stations greatly diminishes the need for precise boundary-depth data. The revised depth data bank used in the new tidal computations are published in Schwiderski (1978a I).

Empirical Tide Data

The new tide model incorporates, by a unique hydrodynamical interpolation procedure (next section), empirical tidal data observed and harmonically analyzed at numerous continental and island stations. These data were taken from publications by the National Ocean Survey (1942), the International Hydrographic Bureau (1966), the British Admiralty (1977 I), and by Pekeris and Accad (1969 I), Zahel (1970 I, 1973 I), Cartwright (1971), and Luther and Wunsch (1975 I). Unfortunately, the most recent publication by the British Admiralty lists harmonic constants only for the four major tide components M_2, S_2, K_1, and O_1 and excludes the European waters completely.

The voluminous data banks had to be screened in order to eliminate observations that are meaningless or unreliable for the present ocean-tide investigations. For example, tidal constants were excluded that were listed for stations deep inside estuaries or narrow bays (e.g., Hudson River, Bay of Fundy), at the mouths of large rivers (e.g., Amazon), between sheltering islands (e.g., Alexander Archipelago, Solomon Islands), and inside sheltering reefs (e.g., Great Barrier Reef).

About 2,500 stations were selected for further examination of their data concerning locally restricted distortions. For instance, some data taken over short distances along a coastline displayed rather drastically alternating times of high water, which are obviously meaningless for oceanic tidal studies. At many stations, different tables give different tidal constants. Some of those discrepancies at island stations are shown for the M_2-tide in Table 1. Similarly, for some mesh cells, several different station data were available, and only one representative average had to be chosen. This situation is illustrated in Table 2 for the M_2-tide around Bermuda. Many of those differences can probably be explained as simple errors in printing or computing. For instance, the phase difference of about 1 hr at Port Galets on La Reunion Island (Table 1) seems to be due to some error in observing the correct reference time, which varies from listing to listing. Most differences, such as those shown for Bermuda stations in Table 2, are definitely true local variations. In this connection, the important tidal measurements by Gallagher *et al.* (1971) at Fanning Atoll in the central Pacific may be men-

Table 1
Empirical M_2-tide differences.

Station Latitude, Longitude		B.A.T.(77)[a] $\xi^b(m)$	$\delta^c(°)$	N.O.S.(42)[d] $\xi(m)$	$\delta(°)$	Others $\xi(m)$	$\delta(°)$	Initialed
Tenerife, Canary Island	(A)	0.67				0.69		Z[e]
28°29′N 16°14′W			18				30	
Port Praia, Cape Verde I.	(A)	0.42				0.43		Z[e]
14°55′N 23°31′W			244				220	
Ascension Island	(A)	0.33				0.51		P,[f]Z
7°55′S 14°25′W			177				174	
St. Helena Island	(A)	0.32				0.34		P,Z
15°55′S 5°42′W			81				87	
Tristan da Cunha Island	(A)	0.23				0.34		P,Z
37°02′S 12°18′W			12				354	
Agalega Island	(I)	0.29				0.29		Z
10°26′S 56°40′E			350				290	
Port Galets, La Reunion I.	(I)	0.16		0.14		0.14		Z
20°55′S 55°17′E			302		328		328	
Mawson, Antarctica	(I)	0.04				0.04		Z
67°36′S 62°53′E			232				155	
Wilkes Station, Antarctica	(I)	0.28				0.38		Z
66°15′S 110°31′E			162				140	
Welles Harbor, Midway I.	(P)	0.11				0.11		P,Z
28°12′N 117°22′W			82				91	
Eniwetok Atoll, Marshall I.	(P)	0.36		0.36				
11°21′N 162°21′E			127		137			
Iles Wallis, Fiji Island	(P)	0.53		0.52				
13°22′S 176°11′W			178		154			
Suva Harbor, Viti Levu, Fiji Island	(P)	0.56		0.50				
18°09′S 178°26′E			196		212			

[a] B.A.T.(77) = British Admiralty Tables (1977 f).
[b] ξ = tidal amplitude.
[c] δ = tidal phase relative to Greenwich.
[d] N.O.S. (42) = National Ocean Survey (1942).
[e] Z = Zahel (1970 f).
[f] P = Pekeris and Accad (1969 f).

tioned. Tides outside and inside the small atoll's lagoon differed by about 50% (20 cm) in amplitude and by a phase lag of about 50° (1 hr, 40 min.).

In general, the most recent listings in the British Admiralty Tide

Tables (1977 I) were chosen over older tabulations as the most reliable. The selection of the data was further aided by earlier and subsequent tidal computations. Altogether, some 1,700 M_2-tide data were selected and assigned to the centers of their respective mesh cells. Using linear interpolation and tidal computations, the total number of prescribed tide data used in the M_2-tide construction was increased to more than 2,000. Essentially all continental boundary cells carry empirically supported tide data. The empirical coverage is only marginal at arctic and antarctic shorelines. Most empirical tide data known at island stations are also included in the tide model.

Naturally, it must be remembered that the selection of representative, empirical tidal data (compare depth data, section before "Hydrodynamically Defined Ocean Bathymetry") is not at all free of subjective judgment and may be somewhat erratic. Obviously, only future additional tidal measurements can improve this model

Table 2
Bermuda M_2-tide observations.

Station Latitude, Longitude	ξ^a(cm)	δ^b(°)	Reference
St. George's Island	36		
32.56N, 64.70W		359	British Admiralty (1977 I)
St. David's Island	34		
32.37N, 64.65W		356	British Admiralty (1977 I)
Great Sound	36		
32.32N, 64.83W		6	British Admiralty (1977 I)
St. George's Island	35		
32.37N, 64.70W		0	National Ocean Survey (1942)
St. George's Island	37		
32.40N, 64.70W		0	Pekeris and Accad (1969 I)
St. George's Island	36		
32.37N, 64.70W		359	Zahel (1970 I)
St. George's Island	36		
32.40N, 64.70W		358	Zettler *et al.* (1975)
Deep Sea (GOBI IV)	36		
32.29N, 64.80W		11	J. T. Kuo Letter (1977)

[a] ξ = tidal amplitude.
[b] δ = tidal phase relative to Greenwich.

in this respect. Nevertheless, according to the instruction notes accompanying the British Admiralty Tide Tables (1977 I), it can probably be assumed that almost all important tide data selected carry an accuracy that is at least as high as the desired 10 cm. In any case, computational experiments showed that isolated reasonable variations of the boundary-tide data do not affect significantly the adjacent oceanic tides. It was also found insignificant to the overall quality of the tide model whether the empirical data were assigned to the centers or to the shore boundaries of the respective cells.

Attempts were made to incorporate also recent deep-sea tidal measurements into the present model. Since the hydrodynamical interpolation of empirical data is essentially based on bottom and boundary irregularities (see next section (a)–(d)), no physically valid justification was found to include distant offshore deep-sea measurements into the model. However, some deep-sea measurements near rough shore and bottom areas were included. Fortunately, without exception, all excluded offshore deep-sea measurements known to the author agree very well with the computed M_2-tide data (see Table 3).

Table 3a
Deep-sea M_2-tide data for the Gulf of Mexico and Caribbean Sea.

Station	Observed		Model		Error	
Latitude, Longitude	ξ^a(cm)	δ^b(°)	ξ(cm)	δ(°)	$\Delta\xi$(cm)	$\Delta\delta$(°)
W. Florida Shelf St.	7		7		0	
26.71N, 84.25W		97		92		−5
Deep Gulf St.	1.3		1.6		+0.3	
24.77N, 89.65W		226		225		−1
Misteriosa Bank	8		9		+1	
18.88N, 83.81W		84		89		+5
Rosalind Bank	7		8		+1	
16.61N, 80.34W		107		102		−5
East Carib. St. (6-month)	0.5		1.6		+1	
16.54N, 64.88W		156		151		−5
East Carib. St. (1-month)	0.6		1.5		0.9	
16.52N, 64.91W		153		148		−5

[a] ξ = tidal amplitude.
[b] δ = tidal phase relative to Greenwich.

Table 3b
Deep-sea M_2-tide data for the Pacific and Atlantic oceans.

Station Latitude, Longitude	Observed ξ^a(cm)	Observed δ^b(°)	Model ξ(cm)	Model δ(°)	Error $\Delta\xi$(cm)	Error $\Delta\delta$(°)
Pacific St. 1 (Middleton)	110		included			
58.76N, 145.71W		284				
Pacific St. 3 (Tofino)	99		included			
48.97N, 127.29W		239				
Pacific St. (San Francisco)	54		included			
38.16N, 124.91W		227				
Pacific St. (Josie II)	27		27		0	
34.00N, 144.99W		267		273		+6
Pacific St. (Flicki)	43		included			
32.24N, 120.86W		149				
Pacific St. (Josie I)	43		included			
31.03N, 119.80W		142				
Pacific St. (Kathy)	29		27		−2	
27.75N, 124.37W		128		130		+2
Pacific St. (Filloux)	19		18		−1	
24.78N, 129.02W		107		105		−2
Atlantic St. 1 (N.Y. Bight)	44		included			
39.32N, 64.36W		350				
Atlantic St. (N.C. St. 1)	48		46		−2	
32.69N, 75.62W		356		358		+2
Atlantic St. (Savannah B)	88		included			
31.95N, 80.68W		15				
Atlantic St. (Scope)	45		46		+2	
30.43N, 76.42W		358		3		+5
Atlantic St. (AOML 1)	34		35		+1	
28.14N, 69.75W		1		6		+5
Atlantic St. (AOML 3)	34		34		0	
28.24N, 67.54W		359		4		+5
Atlantic St. (MERT)	34		34		0	
27.99N, 69.67W		360		6		+6
Atlantic St. (REIKO)	35		34		−1	
27.97N, 69.67W		1		6		+5
Atlantic St. (EDIE-May)	32		32		0	
26.46N, 69.33W		3		7		+4
Atlantic St. (EDIE-March)	31		32		+1	
26.45N, 69.32W		1		7		+6

[a] ξ = tidal amplitude.
[b] δ = tidal phase relative to Greenwich.

Of course, the continuity gap (Equation 4) can be attributed to the following major causes which are physically plausible:

(a) The bottom-friction coefficient, b (in A^4 and B^4 of Equations 62 in Part I), which is most effective in boundary cells, depends on local shore features such as true cell size and bottom slope and roughness.
(b) The boundary cells are idealized by definition of strictly mathematical boundaries (see Figure 1).
(c) The depth data of boundary cells are subjectively defined and, hence, faulty (section, "Hydrodynamically Defined Ocean Bathymetry").
(d) The empirical tidal constants in Equation 3 are also faulty to some degree because of inaccurate measurements, harmonic analyses, and subjective selections and assignments to the centers of the boundary cells (preceding section).
(e) The discrete ocean-tide model is certainly not an exact description of the true oceanic tide; e.g., at boundaries, nonlinear inertial terms assume significance.

Obviously, the last two (hopefully minor) faults can be reduced only through continued future observations and modeling. However, the first two faults, (a) and (b), can be weakened by "hydrodynamically interpolating" the empirical tidal elevations (Equation 3) into the tidal model and narrowing the continuity gap (Equation 4) to an acceptable level as follows:

(A) Adjusting the velocity field by a locally controlled implicit variation of the bottom-friction coefficient, b, in Equations 62 Part I.
(B) Lifting the strict condition of no-flow across the mathematical ocean boundary and allowing for a monitored in- or out-flow by implicitly defining a more physical ocean boundary (Figure 1).

As was pointed out in Part I, section, "The Discrete Ocean-Tide Equations (DOTEs)," due to the choice of the finite-difference

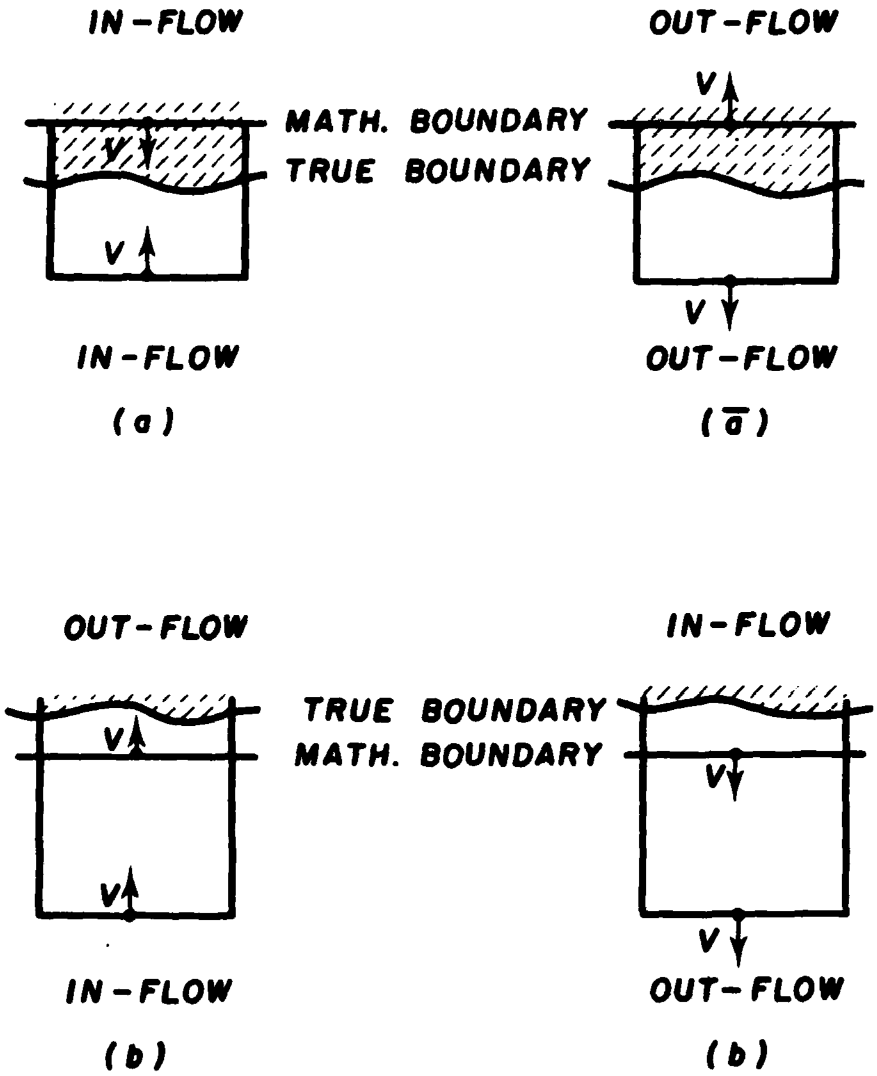

Figure 1. Boundary cell in- and out-flow illustration: (a) and ($\bar{a}$), also (b) and ($\bar{b}$) are half-periods apart. (Shaded region is land area.)

parameter $\kappa = 1$, the bottom friction coefficient, b, in A^4 and B^4 of the momentum equations (Part I, Equations 60) can be considered implicitly varied in the mesh cell $S_{m,n}$ by directly replacing the velocity components in Equation 2 as follows:

$$U^{j+1}_{m,n} \rightarrow U^{j+1}_{m,n} + \left|U^{j+1}_{m,n}\right| (w u_1 + \bar{w} \bar{u}_1),$$

$$U^{j+1}_{m+\mu,n} \rightarrow U^{j+1}_{m+\mu,n} + \left|U^{j+1}_{m+\mu,n}\right| (w u_2 + \bar{w} \bar{u}_2),$$

$$V^{j+1}_{m,n} \rightarrow V^{j+1}_{m,n} + \left|V^{j+1}_{m,n}\right| (w v_1 + \bar{w} \bar{v}_1), \tag{5}$$

and

$$V^{j+1}_{m,n-1} \rightarrow V^{j+1}_{m,n-1} + \left|V^{j+1}_{m,n-1}\right| (w v_2 + \bar{w} \bar{v}_2),$$

provided $\xi_{m,n} \neq 0$; i.e., provided an empirical tidal amplitude is available for the considered mesh cell. In Equation 5, the consistency and scale parameters $(u, \bar{u})$ and $(v, \bar{v})$ are defined by

$$\begin{cases} u_1 = 1, \bar{u}_1 = 0 & \text{for } \Delta\zeta^{j+1}_{m,n} \cdot U^{j+1}_{m,n} < 0, \\ u_1 = 0, \bar{u}_1 = A^4_{m,n} & \text{otherwise, but} \\ u_1 = 0, \bar{u}_1 = 0 & \text{if } \tilde{\xi}_{m-\mu,n} \neq 0; \end{cases} \tag{6a}$$

$$\begin{cases} u_2 = 1, \bar{u}_2 = 0 & \text{for } \Delta\zeta^{j+1}_{m,n} \cdot U^{j+1}_{m-\mu,n} > 0, \\ u_2 = 0, \bar{u}_2 = A^4_{m+\mu,n} & \text{otherwise;} \end{cases} \tag{6b}$$

$$\begin{cases} v_1 = 1, \bar{v}_1 = 0 & \text{for } \Delta\zeta^{j+1}_{m,n} \cdot V^{j+1}_{m,n} < 0, \\ v_1 = 0, \bar{v}_1 = B^4_{m,n} & \text{otherwise;} \end{cases} \tag{6c}$$

and

$$\begin{cases} v_2 = 1, \bar{v}_2 = 0 & \text{for } \Delta\zeta^{j+1}_{m,n} \cdot V^{j+1}_{m,n-1} > 0, \\ v_2 = 0, \bar{v}_2 = B^4_{m,n-1} & \text{otherwise, but} \\ v_2 = 0, \bar{v}_2 = 0 & \text{if } \xi_{m,n-1} \neq 0. \end{cases} \tag{6d}$$

The continuity gap (Equation 4) will be narrowed when the "control parameters" w and $\bar{w}$ are determined successively by:

$$w = \begin{cases} \Delta\zeta^{j+1}_{m,n}/\zeta & \text{for } \zeta \neq 0, \\ 0 & \text{for } \zeta = 0 \end{cases} \tag{7a}$$

with the first "control limit"

$$|w| \leqslant k_1 \tag{7b}$$

and

$$w = \begin{cases} [\Delta\zeta^{j+1}_{m,n} - w\zeta]/\bar{\zeta} & \text{for } \bar{\zeta} \neq 0, \\ 0 & \text{for } \bar{\zeta} = 0 \end{cases} \tag{8a}$$

with the second control limit

$$|w| \leqslant k_1 \tag{8b}$$

where (see Equation 3)

$$\left.\begin{aligned} \zeta &= C^1_n\,[u_1\,|U^{j+1}_{m,n}| + u_2\,|U^{j+1}_{m+\mu,n}|] + v_1C^2_n|V^{j+1}_{m,n}| + v_2C^3_n|V^{j+1}_{m,n-1}| \\ &\text{and} \\ \bar{\zeta} &= C^1_n\,[\bar{u}_1\,|U^{j+1}_{m,n}| + \bar{u}_2\,|U^{j+1}_{m+\mu,n}|] + \bar{v}_1C^2_n|V^{j+1}_{m,n}| + \bar{v}_2C^3_n|V^{j+1}_{m,n-1}|. \end{aligned}\right\} \tag{9}$$

It is important to note that $u_i \cdot \bar{u}_i = 0$ and $v_i \cdot \bar{v}_i = 0$ for $i = 1, 2$. Accordingly, both control limits, k_1 and k_2, which are at one's disposal, regulate the allowed decrease or, respectively, increase of the velocity components in Equations 5; i.e., the implicitly permitted corresponding increase or decrease of the local bottom-friction coefficients. Since the integration sweeps across the ocean from $m = \mu$ to 360 and $n = 4$ to 168, the special choice of $u_1 = \bar{u}_1 = 0$ and $v_2 = \bar{v}_2 = 0$ in Equations 6a and 6d excludes possible double adjustments of the velocity components. Also, if $u_1 \neq \bar{u}_1$ and/or $v_2 \neq \bar{v}_2$, backward adjustments of the tidal elevations via the corresponding Equation 2 must be made. This requires the replacements

$$\left.\begin{aligned} \zeta^{j+1}_{m-\mu,n} &\rightarrow \zeta^{j+1}_{m-\mu,n} - C^1_n|U^{j+1}_{m,n}|(wu_1 + \bar{w}\bar{u}_1) \\ &\text{and} \\ \zeta^{j+1}_{m,n-1} &\rightarrow \zeta^{j+1}_{m,n-1} - C^2_n|V^{j+1}_{m,n-1}|(wv_2 + \bar{w}\bar{v}_2). \end{aligned}\right\} \tag{10}$$

Analogous substitutions in the forward directions of m and n follow automatically in the integration process.

The velocity replacements in Equations 5 may be illustrated by the example

$$\left.\begin{aligned} &U^{j+1}_{m,n} > 0,\ U^{j+1}_{m+\mu,n} > 0,\ V^{j+1}_{m,n} > 0,\ V^{j+1}_{m,n-1} \gtreqqless 0,\\ &\Delta\zeta^{j+1}_{m,n} > \tilde{\xi}_{m-\mu n} = 0,\ \tilde{\xi}_{m,n-1} \neq 0. \end{aligned}\right\} \quad (11)$$

One finds $w > 0, \overline{w} \geqslant 0$, and

$$\left.\begin{aligned} &U^{j+1}_{m,n} \rightarrow U^{j+1}_{m,n}(1 + \overline{w}A^4\ ),\\ &U^{j+1}_{m+\mu,n} \rightarrow U^{j+1}_{m+\mu,n}(1 - w),\\ &V^{j+1}_{m,n} \rightarrow V^{j+1}_{m,n}(1 + \overline{w}B^4_{m,n}), \end{aligned}\right\} \quad (12)$$

and

$$\zeta^{j+1}_{m-\mu,n} \rightarrow \zeta^{j+1}_{m-\mu,n} - C^1_n U^{j+1}_{m,n}\overline{w}A^4_{m,n}.$$

At this point, it must be mentioned that attempts were explored to lift the conrol limits prescribed by k_1 and k_2 in Equations 7b and 8b in an effort to close the continuity gap completely. However, since the bottom-friction coefficient, b, is rather small the control limits, k_1 and k_2, had to be kept small to achieve best results. Computations conducted with large control limits k_1 (excessive bottom friction) seemed to close the continuity gap, but the tidal and velocity fields in the open oceans assumed unrealistically small values. Large control limits k_2 (insufficient bottom friction) produced strong instabilities as anticipated from the analysis in the section, "Stability Analysis," of Part I. To safely check the possible instability, the second control parameter $\overline{w}$ (Equations 5, 6, and 12) was defined in units of $\overline{u} = A^4$ and $\overline{v} = B^4$, in contrast to u = 1 and v = 1, used for the first control parameter w.

After some trial-and-error computations, the following control limits were chosen for the m_2-tide model:

$$k_1 = 0.03,\ k_2 = 0.06. \quad (13)$$

These moderate values reflect the well-known fact that the magnitude of bottom friction has a strong effect on the motions considered. Indeed, with some minor improvements of the tidal field, significant improvements of the continuity gap, velocity field, and convergence of the integration were achieved. This procedure was applied to all oceanic cells with known empirical tide data (Equation 3), provided these cells bordered terrestrial cells or contained small islands or other bottom irregularities. No meaningful reason was seen to apply the same bottom-friction adjustment procedure to distant offshore oceanic cells with available deep-sea tide measurements.

In order to implement the second step (B) of the hydrodynamical interpolation procedure, the following velocity replacements in oceanic mesh cells bordering terrestrial cells were defined:

$$\left.\begin{aligned} U^{j+1}_{m,n} &\to \tilde{w}\tilde{u}_1 U^{j+1}_{m+\mu,n}, \\ U^{j+1}_{m+\mu,n} &\to \tilde{w}\tilde{u}_2 U^{j+1}_{m,n}, \\ V^{j+1}_{m,n} &\to \tilde{w}\tilde{v}_1 V^{j+1}_{m,n-1} \\ \text{and} \qquad & \\ V^{j+1}_{m,n-1} &\to w v_2 V^{j+1}_{m,n}, \end{aligned}\right\} \tag{14}$$

provided $\tilde{\xi} \neq 0$ in Equation 3. The parameters $(\tilde{u}\tilde{v})$ are mutually consistent by definition:

$$\left.\begin{aligned} \tilde{u}_1 &= 1 \text{ if } U^{j+1}_{m,n} = 0, \text{ otherwise } \tilde{u}_1 = 0, \\ \tilde{u}_2 &= 1 \text{ if } U^{j+1}_{m+\mu,n} = 0, \text{ otherwise } \tilde{u}_2 = 0, \\ \tilde{v}_1 &= 1 \text{ if } V^{j+1}_{m,n} = 0, \text{ otherwise } \tilde{v}_1 = 0, \\ \text{and} \qquad & \\ \tilde{v}_1 &= 1 \text{ if } V^{j+1}_{m,n-1} = 0, \text{ otherwise } \tilde{v}_2 = 0. \end{aligned}\right\} \tag{15}$$

The remaining continuity gap will be further narrowed when the control parameter $\tilde{w}$ is determined to be in agreement with Equations 2, 4, 7, 8, and 9 by

$$\tilde{w} = \begin{cases} [\Delta\zeta^{l+1}_{m,n} - w\zeta - \overline{w}\overline{\zeta}]/\tilde{\zeta} & \text{for } \tilde{\zeta} \neq 0 \\ 0 & \text{for } \tilde{\zeta} = 0 \end{cases} \quad (16a)$$

with the third control limit

$$|\tilde{w}| \leq k_3, \quad (16b)$$

where

$$\tilde{\zeta} = C^1_n[\tilde{u}_1 U^{l+1}_{m+\mu,n} - \tilde{u}_2 U^{l+1}_{m,n}] + \tilde{v}_1 C^2_n V^{l+1}_{m,n-1} - \tilde{v}_2 C^3_n V^{l+1}_{m,n}. \quad (17)$$

Obviously, the substitutions (Equations 14) specify consistent in- or out-flows across the mathematical boundaries of oceanic coastal cells, as illustrated in Figure 1, without explicitly fixing the physical boundary line. Again, no complete removal of the continuity gap was possible. The most satisfactory results for the M_2-tide were achieved by setting the third control limit (Equation 16b) at

$$k_3 = 0.5. \quad (18)$$

While the improvement of the tidal field was again moderate, the remaining continuity gaps and nearshore velocity distortions assumed uniformly satisfactory levels. The remaining small shortcomings of the model can easily be attributed to the boundary inaccuracies (c), (d), and (e) listed above, but for which no simple remedies were found.

It may be emphasized that the rather significant change in the nearshore velocity field permitted by the in- and out-flow specifications (Equations 14) affected the tidal field only in a minor fashion. This important phenomenon is in agreement with the well-known fact that the pressure distribution in a fluid motion is very insensitive to large but local velocity variations. For instance, it is perhaps the most important postulate in Prandtl's boundary-layer theory (see, e.g., Schlichting, 1968 I), and it is the basis of the hydrostatic-pressure assumption invoked here and in the section, "The Continuous Ocean-Tide Equations (COTEs)," of Part I for the present tidal model.

The hydrodynamical interpolation technique considerably accelerated the convergence of the integration procedure toward the steady state amplitudes and phases. In fact, the computation of the new M_2-tide model (sections, "Quality of the Ocean-Tide Model" and "Conclusions") was terminated when the amplitudes and phases over all open ocean areas differed by less than 1 cm and 1°, respectively. Obviously, this improved convergence feature goes significantly beyond the same property described in Part I, section, "Lateral-Boundary, Initial and Final Data," for the purely mathematical model.

Quality of the Ocean-Tide Model

Since the present tide model incorporates essentially all known empirical data by hydrodynamical interpolation (preceding section), no direct comparison of observed and computed data is feasible. Nevertheless, a comprehensive appraisal of the reality of the present tide model is possible by inspecting the quality of hydrodynamical interpolation; i.e., by evaluating the "smoothness" with which the computed tide "accepts or rejects" the empirical tidal data. In fact, the smoothness characteristics of the novel hydrodynamical interpolation technique are distinctly different from those of other direct interpolation procedures using power or trigonometric polynomials. In the latter case, smoothness of the interpolation can be carried up to any desired degree by simple design. The adjustment of hydrodynamical parameters (preceding section) in the former method does not imply any smoothness of the interpolation, unless both the empirical input data and the hydrodynamical tide model are compatible with each other.

As is well known, local tidal distortions, caused by an isolated roughness (seamount or small island) in the bottom relief, affect the surrounding ocean tide very little. The major level of ocean tides is shaped by continental shorelines and large (in area and/or length) islands and ridges. In contrast to ordinary polynomial interpolations, an important feature of the new hydrodynamical interpolation method is that it preserves those significant properties of ocean tidal currents without any essential alterations.

Extensive computer experiments were conducted to test the important smoothness characteristics of the hydrodynamical interpolation procedure. Faulty input data were deliberately inserted and quickly recognized as rejected by the computed surrounding tide. Indeed, the first computations, which included empirical tidal data, revealed immediately several input errors in the data. Vice versa, smoothly accepted empirical tidal data were randomly deleted to test their backlash reaction on the computed tide. As anticipated, no significant modifications were detected. Consequently, the hydrodynamical interpolation technique permits a check of the reality of both the tide model and the empirical tidal input data. If an input value is rejected by the computed tide, then one or the other or both are defective. Fortunately, only very few discrepancies between the different sources of observed M_2-tide data (see section, "Empirical Tide Data") have been discovered that way.

The new discrete tide-model has been applied to compute the global M_2 ocean tide. A complete discussion and tabulation of all amplitudes and phases is presented in Schwiderski (1979c I). In order to display the quality of the tidal model, the computed amplitudes (in cm) and phases (in degrees) along with their adjacent empirical values have been tabulated in "30° by 50° map form" for four typical ocean areas (Tables 4–7). All empirically supported input data along continental shores and at island stations are underlined in the tables. All nearshore deep-sea measurements included in the model are labeled by subbrackets. As was explained in the preceding section, all distant offshore deep-sea measurements are not included in the tide model. However, their approximate locations are marked by wavy underlines, and their corresponding observed data are listed in Table 3. Land points are left blank.

In the evaluation of the tidal accuracy, one must remember that the ocean tide at any fixed location is determined by two harmonic constants. If (ξ_0,δ_0) and (ξ,δ) denote the respective local amplitudes and phases of the "true" and "computed" tides

$$\zeta_o = \xi_0 \cos(\sigma t - \delta_0),\ \zeta = \xi \cos(\sigma t - \delta), \tag{19}$$

then their time-dependent error is

$$\tilde{\zeta} = \zeta_0 - \zeta = \tilde{\xi} \cos(\sigma t - \tilde{\delta}) \tag{20}$$

with the standard deviation

$$\mathrm{rms}(\tilde{\zeta}) = \tfrac{1}{2}\sqrt{2}\tilde{\xi}, \tag{21}$$

where

$$\tilde{\xi}^2 = \xi_0^2 - 2\xi_0\xi \cos(\delta_0 - \delta) + \xi^2 \tag{22}$$

and

$$\tan \tilde{\delta} = \frac{\xi_0 \sin \delta_0 - \xi \sin \delta}{\xi_0 \cos \delta_0 - \xi \cos \delta}. \tag{23}$$

Some maximum errors are

$$\tilde{\zeta}_M = \tilde{\xi}_M = \xi_0 + \xi \text{ for } \delta_0 - \delta = 180°, \tag{24}$$

$$\tilde{\zeta}_M = \tilde{\xi}_M = \xi_0 - \xi \text{ for } \delta_0 - \delta = 0°, \tag{25}$$

$$\tilde{\zeta}_M = \tilde{\xi}_M = 2\xi \sin \tfrac{1}{2}(\delta_0 - \delta) \text{ for } \xi = \xi_0, \tag{26}$$

and

$$\tilde{\zeta}_M = \tilde{\xi}_M = \xi \text{ for } \xi = \xi_0 \text{ and } \delta_0 - \delta = 60°. \tag{27}$$

Equation 27 expresses the important fact that a 60° phase error results in an amplitude error equal to the tidal amplitude and, hence, renders the computed tidal prediction completely useless. Of course, in regions of sufficiently small amplitudes, any phase error is acceptable.

Tables 4A and 4B depict the tidal amplitudes and phases, respectively, of the northwestern Atlantic Ocean including the eastern Caribbean Sea. As can be verified by earlier tide models, this entire area was very difficult to model, because its rough bottom topography has a strong effect on the tidal currents that sweep over or across various barriers with rapidly changing water levels. There is the broad and shallow continental shelf along the whole North American shoreline, with Cape Hatteras, Long Island, Cape Cod, Nova Scotia, and Newfoundland all protruding into the ocean basin. Furthermore, there are the Grand Banks, the Bahama Banks, and the long and narrow Caribbean Ridge. Obviously, all of the corresponding local tidal features could not be realistically captured by the tide model without a proper representation of the bathymetry (section, "Hydrodynamically Defined Ocean Bathymetry") and without the hydrodynamical interpolation (preceding section) of the locally collected tidal observations.

Now, if one scans the tidal amplitudes and phases (Tables 4A and 4B) from the north to the south, one gathers the impression that the whole computed ocean tide is completely locked into the array of empirical (underlined) tidal data everywhere along the continental coast and along the many aligned islands separating the Atlantic Ocean from the Gulf of Mexico and the Caribbean Sea. It is particularly impressive to see the observed tide data at the offshore islands (Sable—SI, Barbados—BB, and even as far as Bermuda—BI) and at the included nearshore (subbrackets), deep-sea stations all realistically well-accepted by the computed surrounding tide. Moreover, one finds the excluded offshore deep-sea measurements (locations marked by wavy underlines) in the Atlantic and Caribbean Sea fully verified by the independent tide model.

As can be seen in the special listing of Table 3, the measured and computed amplitudes and phases at the Atlantic stations agree within 2 cm and 6°, respectively. The remaining discrepancy is probably within the experimental error due to short observation times and the use of the distant reference station Bermuda (Zettler *et al.*, 1975), which exhibits even larger gaps between the various tidal observations listed in Table 2.

Attention may be drawn to the existence of considerable slopes between the empirical boundary data and the computed ocean-tide values in the high-amplitude ranges from Nova Scotia to Cape Cod and from Cape Hatteras to Florida's coast. Yet, these rapid tidal variations can be considered as realistic because throughout the same sections the empirical data, among themselves, display exactly the same roughness. This only substantiates clearly the fundamental difference between polynomial and hydrodynamical interpolation techniques pointed out above.

In the complete report (Schwiderski, 1979c I), the same tidal roughness will be recognized in several similar coastal places around the world. From this typical phenomenon, one can draw the fortunate conclusion that, while some empirical data may be lacking high accuracy (see Table 1 and the British Admiralty Tide Tables, 1977 I), the computed adjacent ocean tide may retain its high quality.

In order to gain a deeper insight into the detailed tidal phenomena from the enclosed table charts (e.g., Tables 4A and 4B), it is helpful to recall the physical meaning of the tabulated tidal constants. The local tidal amplitude, ξ, is defined as half the tidal "range," which measures the total variation of the water level from high to low. Lines of constant amplitudes are called "corange lines." The local phase, δ, specifies the tidal cresting time (in degrees) after the moon's (or sun's) passage over the Greenwich meridian. For the present M_2-tide one has the following time conversions:

$$\begin{aligned} 360^\circ &= 12.421 \text{ hr (period)}, \\ 30^\circ &= 1.035 \text{ hr}, \\ 1^\circ &= 2.070 \text{ min}. \end{aligned} \tag{28}$$

Lines of constant phases (simultaneous cresting times) are called "cotidal lines." In particular, at the $0^\circ = 360^\circ$ cotidal lines, which are conspicuously visible in the phase charts (Tables 4B to 7B), the tide crests simultaneously with the moon's passage over the Greenwich meridian. The tidal crest advances with time normal to the cotidal lines toward larger phases. A point of zero amplitude ($\xi = 0$) around which the tidal crest rotates from 0° to 360° is called an "amphidromic point"; it is marked in the tables by a circled star ⊛.

Key to M_2-tide Tables 4–7.

M = Longitude east (°).
N = Colatitude (°).
☆ = Amphidromic point.
— = Subbars mark empirical input data.
└┘ = Subbrackets mark input nearshore deep-sea measurements.
~ = Wavy underlines mark offshore deep-sea tide gauge stations with excluded measurements listed in Table 3a, b.

Table 4A. M_2 tidal amplitudes ξ (cm) of the northwestern Atlantic Ocean.

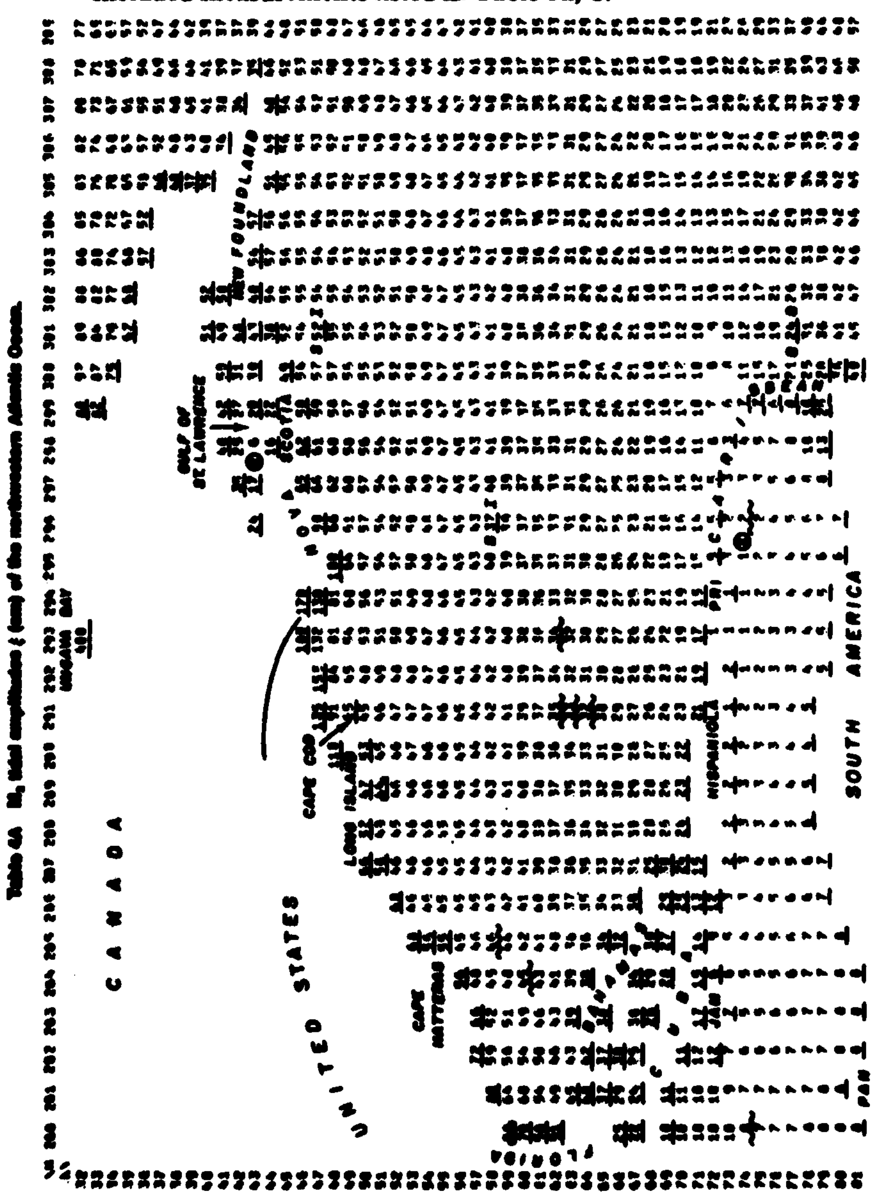

Table 48 M_2 tidal phases δ (°) of the northwestern Atlantic Ocean.

	280	281	282	283	284	285	286	287	288	289	290	291	292	293	294
32														UNGAVA BAY 78	
33															
34															
35															
36					CANADA										
37															
38															
39															
40															
41															
42															
43															
44				UNITED STATES											
45															
46														96	82
47									CAPE COD			102	98	71	62
48											181	95	76	62	60
49								LONG ISLAND				65	37	28	14
50								357	357	357	6	18	12	10	7
51								355	355	355	3	5	6	6	6
52							354	357	358	360	2	3	4	5	4
53						353	356	357	358	360	1	2	3	4	4
54				CAPE HATTERAS		351	357	358	359	0	1	2	3	3	4
55						352	357	358	359	0	1	2	3	4	4
56					358	355	357	359	360	1	2	3	3	4	4
57			354	354	356	357	359	360	1	2	3	3	4	4	5
58		6	358	357	358	358	359	1	2	3	3	4	4	5	5
59	15	1	1	2	2	1	1	2	3	3	4	5	5	5	4
60	22	7	6	5	3	2	3	4	4	5	5	6	6	5	5
61	11	10	8	6	3	5	5	5	6	6	6	7	7	7	5
62	11	13	12	9	8	7	7	7	7	7	7	4	5	5	4
63		13	16	10	10	10	9	9	9	9	8	3	3	4	4
64	FLORIDA	16	12		5	11	11	11	13	10	10	2	5	6	5
65		21	19	9		7	17	13	12	11	11	9	8	6	7
66	42	29	15			28	16	16	13	14	13	12	11	10	9
67	31	31	26	18	12	4	20	18	17	16	15	14	13	12	10
68				21	15	12	3	19	18	18	17	16	16	14	13
69	73	72		CUBA	17	17	15	16	18	19	20	19	19	16	15
70	76	76	72				16	16	13	20	21	22	22	22	21
71	76	75	67	55	58	65	40	34				22	19	20	18
72	84	81	87	JAM	88	65	58	HISPANIOLA						65	PRI
73	91	87	87	102	74	63	51	68	94	109	115	115	73	83	52
74	103	102	102	102	96	92	91	102	111	119	125	129	133	135	162
75	116	116	116	115	112	111	111	113	117	125	131	126	144	157	158
76	131	129	127	126	122	121	120	121	125	129	134	141	149	150	168
77	142	137	134	132	129	126	125	126	128	131	137	147	151	150	160
78	147	142	138	135	132	129	127	127	130	138	161	161	155	161	165
79	152	146	140	130	133	130	128	124					159	157	152
80	155	148	142	137	134	137									
81	180	PAN	141	139	138			SOUTH AMERICA							

	295	296	297	298	299	300	301	302	303	304	305	306	307	308	309
32					317	309	306	304	302	300	297	295	292	285	286
33					315	310	307	305	301	301	295	296	294	291	288
34						313	310	308	305	303	301	299	296	293	290
35							309	305	309	306	301	301	298	295	297
36									304	303	304	303	300	298	295
37											302	305	303	301	298
38											301	308	306	304	307
39											300	311	309	306	307
40							71	62			301	310	310	310	310
41				131	91	79	64	57				303	311	312	314
42			190	110	65	49	70		NEWFOUNDLAND				300	315	318
43		242	201	331	319	5	7	5	3	349				315	323
44				296	351		359	3	359	355	341	332	326	332	328
45			SCOTIA			356	0	358	356	354	359	351	351	350	352
46	NOVA		359	354	354	357	356	355	354	353	351	353	353	352	353
47		33	355	353	356	355	352	354	356	356	356	356	354	354	353
48	31	357	356	355	355	355	355	355	355	355	355	355	355	355	355
49	5	1	359	358	357	357	357	357	357	357	357	357	357	357	357
50	5	3	1	360	359	358	358	358	358	358	358	358	358	358	359
51	4	3	2	1	0	360	359	359	359	359	359	359	359	360	0
52	4	3	2	2	1	0	360	360	360	360	360	360	0	1	1
53	3	3	3	2	2	1	1	0	0	0	0	1	1	2	2
54	4	3	3	2	2	2	1	1	1	1	1	1	2	2	3
55	4	4	3	3	2	2	1	1	1	1	1	1	2	2	3
56	5	5	4	3	3	2	2	1	1	1	1	1	2	2	2
57	5	6	5	4	3	2	2	1	1	1	1	1	1	2	2
58	4	3	4	3	3	2	1	1	1	1	1	1	1	1	1
59	3	3	3	3	2	2	1	1	1	1	0	0	0	0	0
60	4	4	3	3	2	2	1	1	0	0	360	359	359	359	359
61	4	4	3	3	2	1	1	0	360	359	359	358	358	357	357
62	4	4	3	2	2	1	0	360	359	358	357	356	356	355	355
63	4	4	3	2	1	1	360	355	358	356	355	354	353	352	352
64	5	4	4	2	1	0	359	358	356	355	351	357	350	349	349
65	6	5	3	2	1	359	358	356	354	353	351	349	347	346	344
66	7	6	4	2	0	358	356	354	352	350	347	345	343	341	339
67	9	7	5	2	359	355	353	351	348	345	343	340	337	335	333
68	11	9	5	2	358	354	350	347	343	340	336	333	330	328	325
69	14	11	6	1	356	350	345	340	335	331	327	324	321	318	314
70	17	13	9	1	352	346	336	329	323	319	315	312	309	306	304
71	22	19	15	3	347	339	321	313	308	303	300	298	295	293	291
72	11	21	359	355	332	311	299	295	288	286	284	283	281	280	279
73	220	4	318	308	290	281	276	272	271	270	269	269	269	269	268
74	95	152	257	267	250	250	257	256	257	257	255	259	259	260	259
75	187	212	270	210	238	244	244	245	247	248	250	251	252	253	253
76	180	193	207	206	219	229	235	238	240	242	244	245	246	247	247
77	177	187	197	204	217	227	224	229	236	238	239	240	241	242	241
78	175	193	194	202	217	221	236	233	234	236	234	237	238	239	240
79	173	170	208	210	216	218	231	230	231	232	233	236	236	237	237
80	150	182				220	229	228	229	230	231	232	233	234	235
81						229	226	225	227	225	230	231	231	233	233

Table 8A M_2 tidal amplitudes ξ (cm) of the northeastern Pacific Ocean.

φ \ λ	216	217	218	219	220	221	222	223	224	225	226	227	228	229	230	231	232	233	234	235	236	237	238	239	240	241	242	243	244	245
30						ALASKA																								
31	112	112	112	112	111																									
32	108	108	108	108	111	111	110																							
33	104	104	105	106	107	109	110	110	112																					
34	100	101	102	104	105	107	109	111	111	115																				
35	96	97	99	100	102	103	105	107	110	113	123						CANADA													
36	92	93	95	96	98	100	101	103	104	109	111	122	106	QUEEN																
37	88	89	91	92	94	95	97	99	101	103	106	116		CHARLOTTE I.																
38	84	85	87	88	90	92	93	95	97	98	100	101	100		120	135														
39	80	81	83	85	86	88	89	91	93	94	95	96	101	112	119	111	124													
40	76	78	79	81	82	84	85	87	89	90	92	94	97	100	102	103	106													
41	73	74	76	77	79	80	82	83	85	86	88	89	92	94	96	98	98	102	99											
42	69	71	72	74	75	76	78	79	81	82	83	85	87	89	91	92	93	99	91	88										
43	66	68	69	70	71	73	74	75	77	78	79	81	83	84	86	87	88	89	89	90	86				UNITED					
44	63	64	65	67	68	69	71	72	73	74	76	77	79	80 C	81 S	85	85	86	87	89	86									
45	60	61	62	63	64	66	67	68	69	71	72	73	75	76	78	79	81	82	84	86	83				STATES					
46	57	58	59	60	61	63	63	64	66	67	69	70	71	77	74	75	77	79	80	83	86									
47	54	55	56	57	58	59	60	61	62	64	65	66	67	68	70	71	72	74	75	77	76									
48	52	53	53	54	55	56	57	58	59	60	61	62	63	64	65	64	67	68	70	71	74									
49	49	50	50	51	51	52	54	55	55	56	57	58	59	59	60	61	62	63	66	65	71									
50	46	46	47	48	48	49	50	51	52	52	53	53	54	55	56	57	58	59	60	60	63									
51	43	44	44	45	45	46	47	47	48	48	49	49	50	51	51	52	53	54	56	57	68									
52	41	41	41	42	42	43	43	44	44	44	45	45	46	46	47	48	49	51	52	54	63	55	S. FRANCISCO							
53	38	38	39	39	39	39	40	40	40	41	41	41	42	42	43	44	45	46	48	50	57 F	51 I	53							
54	35	35	36	36	36	36	36	36	37	37	37	37	38	38	39	40	41	42	44	45	67	68	49							
55	33	32	32	32	33	33	33	33	33	33	33	34	34	34	35	36	37	38	39	41	62	44	45	49						
56	30	29	29	29	30	30	30	30	30	30	30	30	30	30	31	32	33	34	35	36	40	40	41	63	49					
57	26	26	26	26	27	26	26	26	26	26	26	26	26	27	27	28	29	30	31	31	34	36	38	39	40	49	50			
58	26	24	24	24	24	23	23	23	23	22	22	22	22	23	23	24	25	26	28	29	31	33	35	36	41	44	46	50		
59	21	21	21	21	21	20	20	19	19	19	18	18	18	19	20	21	22	23	25	26	28	31	34	36	39	41	44	49	MEXICO	
60	19	19	18	18	17	17	16	16	15	15	15	15	15	15	16	17	19	20	22	24	26	29	32	36	39	42	43	46	58	
61	17	16	16	15	14	14	13	12	12	11	11	11	11	12	13	14	14	18	20	27	24	28	31	34	37	43	43	45	47	58
62	15	14	14	13	12	11	10	9	9	8	7	7	8	9	10	12	16	15	17	22	29	27	31	34	37	39	42	44 G	51 I	50 31
63	14	13	12	11	9	6	7	6	5	4	4	4	6	7	9	11	12	14	18	21	24	28	31	34	37	39	42	45	46	52
64	12	12	10	9	8	7	4	4	2	1	1	3	5	7	9	10	17	16	20	25	27	29	32	34	37	39	42	45	48	47
65	12	11	10	9	8	7	5	4	3	3	4	5	7	9	11	12	15	19	24	26	28	30	32	36	37	39	42	44	47	50
66	12	11	10	9	4	6	7	7	5	7	7	8	10	11	13	17	20	22	24	26	28	30	32	35	37	39	41	44	46	48
67	13	12	12	11	11	10	10	10	10	10	11	12	13	14	16	19	21	23	25	27	29	31	33	35	37	39	41	43	45	47
68	14	14	13	13	13	13	13	13	13	13	14	15	16	17	19	21	23	24	26	29	30	31	33	35	37	39	40	42	44	45
69	16	15	15	15	15	15	15	16	16	16	17	18	19	20	21	22	24	26	27	29	31	32	33	35	37	38	40	41	42	43
70	18	17	17	17	18	18	18	19	19	19	20	21	21	22	24	25	26	27	29	30	31	33	34	35	37	38	39	40	41	41
71	20	20	20	20	20	20	21	21	22	22	23	23	24	25	26	27	29	29	30	31	32	34	35	36	37	38	38	39	40	40
72	22	22	22	22	22	23	23	24	24	25	25	26	26	27	28	29	30	31	32	33	34	34	35	36	37	37	38	38	39	39
73	24	24	24	24	24	25	25	26	26	27	27	28	29	29	30	31	31	32	33	34	35	35	36	37	37	38	38	38	38	37
74	25	25	26	26	27	27	28	28	29	29	30	30	31	31	32	33	33	34	35	35	36	36	37	37	38	38	38	37	37	36
75	27	27	28	28	29	29	30	30	31	31	32	32	33	33	34	34	35	35	36	37	37	37	38	38	38	38	37	37	36	36
76	29	29	30	30	31	32	32	32	33	33	34	34	35	35	36	36	36	37	37	38	38	38	38	38	38	38	37	37	36	35
77	30	31	32	32	33	34	34	35	35	35	36	36	36	37	37	38	38	38	39	39	39	39	39	39	38	39	37	36	35	34
78	32	33	34	34	35	36	36	37	37	37	36	38	38	39	39	40	40	40	40	40	40	40	40	39	39	38	37	36	35	37
79	34	34	35	36	37	38	38	38	39	39	40	40	41	41	41	41	41	41	41	41	41	41	41	40	39	39	38	36	35	33

Table 5B M2 tidal phases δ (°) of the northeastern Pacific Ocean.

°N \ °W	216	217	218	219	220	221	222	223	224	225	226	227	228	229	230	231	232	233	234	235	236	237	238	239	240	241	242	243	244	245	
30																															
31	283	282	282	281	280																										
32	284	281	282	281	280	279	279																								
33	285	283	282	281	280	279	278	278	277																						
34	284	283	281	280	279	279	277	275	274	273																					
35	283	282	280	279	277	276	274	272	271	269	269																				
36	282	281	279	277	275	274	272	270	268	266	263	266	271																		
37	281	279	277	275	274	272	270	268	267	265	262	259																			
38	279	277	275	274	272	270	268	267	265	263	261	259	255		262	251															
39	278	276	274	272	270	269	267	265	263	261	260	258	256	258	253	250	248														
40	278	274	272	271	269	267	265	263	261	260	258	256	254	252	250	248	245														
41	275	273	271	269	267	266	264	262	260	258	256	254	252	250	248	246	244	243	241												
42	274	272	270	268	266	264	262	260	259	257	255	253	251	249	247	245	243	239	239	240											
43	273	271	269	267	265	263	261	259	257	255	253	251	249	247	245	243	241	240	239	236	238										
44	272	271	268	266	264	262	260	258	256	254	252	250	248	246	244	242	240	239	238	237	236										
45	271	269	267	265	263	261	259	257	255	253	251	249	247	245	243	241	239	237	235	234	235										
46	270	269	268	264	262	260	258	256	254	252	250	248	245	243	241	239	237	235	233	231	233										
47	270	268	266	263	261	259	257	255	253	251	249	246	244	242	239	237	235	232	230	228	226										
48	269	267	265	263	261	258	256	254	252	250	247	245	242	240	237	235	233	230	227	224	216										
49	269	267	264	262	260	258	255	253	251	248	246	243	241	238	235	233	230	227	225	222	212										
50	269	267	264	262	259	257	254	252	249	247	244	241	238	236	233	230	227	225	222	220	212										
51	269	267	264	261	259	256	254	251	248	245	242	239	236	233	230	228	225	222	220	218	212										
52	269	267	264	262	259	256	253	250	247	244	241	238	235	232	228	226	223	220	217	215	227	212									
53	270	264	265	262	259	256	253	250	247	243	240	237	233	230	226	223	220	217	213	209	205	199	212								
54	271	268	266	262	259	256	253	249	246	242	239	235	231	228	224	220	217	213	209	205	206	195	183								
55	273	270	266	263	260	256	253	249	245	241	238	234	229	225	221	217	213	209	205	200	195	189	183	173							
56	275	271	268	264	260	256	253	249	245	241	236	232	227	223	219	214	209	205	200	195	189	184	178	172	162						
57	272	272	268	265	261	257	253	249	245	240	236	231	226	221	215	210	205	200	195	189	184	178	173	167	161	151	146				
58	276	273	270	266	263	259	254	250	245	240	235	229	223	217	211	205	200	194	188	183	177	172	167	161	156	148	144	143			
59	278	276	273	269	265	261	256	251	245	239	234	227	219	212	205	198	192	187	181	175	170	165	160	155	156	142	142	139			
60	282	279	276	272	269	263	258	253	246	240	232	224	215	206	197	190	183	177	172	166	161	157	153	150	146	142	139	137	137		
61	288	285	282	278	273	269	262	256	248	240	231	220	206	197	187	179	172	168	160	156	151	149	145	143	141	138	136	135	134	135	
62	295	297	290	286	282	276	269	261	252	240	226	211	195	182	172	164	158	152	147	144	141	139	130	136	135	134	133	132	132	132	133
63	304	302	301	298	295	290	283	274	261	241	213	186	159	150	151	145	140	135	133	132	130	130	131	130	136	129	129	129	128	131	
64	316	315	315	315	314	313	311	307	33[illegible]	260	141	132	130	128	126	123	120	117	119	121	123	124	125	125	125	125	129	125	125	124	
65	330	330	331	334	339	343	350	1	21	51	77	92	100	104	106	105	139	112	114	116	118	119	120	120	121	121	122	122	122	122	
66	344	346	345	353	359	6	15	26	39	53	67	77	85	92	96	103	106	108	109	111	113	114	115	116	117	118	118	119	119	119	
67	356	359	3	7	13	19	27	36	45	54	63	71	79	85	91	97	100	102	104	106	108	110	111	112	113	114	115	116	117	117	
68	7	9	13	17	22	28	34	41	48	55	62	68	74	80	85	90	93	96	99	101	103	105	107	108	110	111	113	113	114	114	
69	15	17	20	24	28	33	38	44	49	55	61	66	71	76	81	85	88	91	94	96	99	101	103	105	106	108	110	111	112	112	
70	21	24	26	29	33	37	41	46	50	55	60	64	69	73	77	80	84	87	90	92	94	97	99	101	103	105	107	108	109	110	
71	27	28	31	33	36	40	43	47	51	55	59	62	66	70	73	77	80	83	86	88	91	93	95	97	99	102	104	105	106	108	
72	30	32	34	36	39	41	44	48	51	54	57	61	64	67	70	74	77	80	82	85	87	89	91	93	96	98	101	102	104	105	
73	33	35	36	38	40	42	45	48	51	53	56	59	62	65	68	71	74	76	79	81	83	85	88	90	92	95	97	99	101	102	
74	36	37	38	40	41	43	45	47	50	52	55	58	60	63	66	68	71	73	75	78	80	82	84	86	89	91	94	96	98	99	
75	37	38	39	40	42	43	45	47	49	51	54	56	59	61	63	66	68	70	72	74	77	79	81	83	86	88	91	93	94	97	
76	38	39	40	41	42	43	45	47	49	51	53	55	57	59	61	63	65	67	69	72	74	76	78	80	83	85	87	90	92	94	
77	39	40	41	42	43	44	45	46	48	50	51	53	55	57	59	61	63	65	67	69	71	73	75	77	79	82	84	87	89	91	
78	40	41	41	42	43	44	45	46	47	49	51	52	54	56	57	59	61	63	64	66	68	70	72	74	76	79	81	84	86	88	
79	41	41	42	42	43	44	44	46	47	48	50	51	53	54	56	57	59	60	62	64	66	68	70	72	74	76	78	81	83	85	

ALASKA

CANADA

QUEEN CHARLOTTE I.

UNITED STATES

S. FRANCISCO

MEXICO

Table 8A M_2 tidal amplitudes ξ (cm) of the north-central Pacific Ocean.

	177	178	179	180	181	182	183	184	185	186	187	188	189	190	191	192	193	194	195	196	197	198	199	200	201	202	203	204	205	206
30	29	28	28	27	27	27	27	28	29	28	27	25	23	22	23	24	24	28						A L A S K A						
31	28	28	27	27	27	27	27	27	27	27	28	29	28	27	27	27	30	33	33	53	72	81								
32	27	27	26	26	26	26	26	26	26	26	27	27	28	31	28	26	24	24	23	[illegible]	75	31	88	88	150					
33	26	26	26	25	25	25	25	25	25	25	25	26	27	P 26 F	25	25	23	22	19	14	8	7	23	49	84				102	
34	25	25	24	24	24	24	23	23	23	23	23	23	23	27	23	23	23	23	22	19	15	11	25	32			97	88	93	98
35	24	23	23	23	22	22	22	22	22	21	21	21	21	22	22	23	23	24	26	25	26	K A N		P E N I N S U L A		75	83	87	83	84
36	22	22	21	21	21	21	21	21	20	20	19	18	19	20	21	21	22	23	24	A L	A S		66	62	68	72	73	76	75	77
37	21	20	20	20	20	20	20	19	19	19	17	14	15	17	20	U	T I	A N	S	30	44	58	54	57	59	62	65	67	69	71
38	19	19	18	18	18	18	19	19	21	L	E	9	17	23	32	37	37	37	37	39	42	45	49	52	54	57	60	62	64	66
39	17	21	18	15	16	19	24	A	22	25	24	23	25	27	29	31	33	34	36	37	40	43	45	48	51	53	55	58	60	62
40	15	15	15	15	15	16	17	18	20	20	21	22	23	25	27	29	30	32	34	36	38	40	42	45	47	50	52	54	56	58
41	13	13	13	13	13	14	15	16	17	18	19	20	22	23	25	27	28	30	32	34	36	38	40	43	45	47	49	51	53	56
42	11	11	11	11	11	12	13	14	15	16	18	19	21	22	24	25	27	29	31	33	35	37	39	41	43	45	47	49	51	53
43	9	9	9	9	10	11	12	13	14	15	17	18	20	21	23	24	26	28	30	31	33	35	37	39	41	43	45	47	49	51
44	8	8	8	8	9	9	10	12	13	14	16	17	19	20	22	23	25	27	28	30	32	34	36	37	39	41	43	45	47	49
45	7	7	7	7	8	8	9	11	12	13	15	16	18	19	21	22	24	26	27	29	31	32	34	36	38	40	41	43	45	47
46	6	6	6	6	7	7	9	10	11	13	14	16	17	19	20	22	23	25	26	28	30	31	33	35	36	38	40	42	43	45
47	5	5	5	5	6	7	8	9	11	12	13	15	16	18	19	21	22	24	25	27	28	30	32	33	35	37	38	40	41	43
48	5	4	4	4	5	6	7	9	10	11	13	14	16	17	19	20	21	23	24	26	27	29	30	32	34	35	37	38	40	41
49	4	4	4	4	5	6	7	8	9	11	12	13	15	16	18	19	21	22	23	25	26	28	29	31	32	34	35	37	38	39
50	4	3	3	3	4	5	6	7	9	10	11	13	14	15	17	18	20	21	22	24	25	26	28	29	31	32	34	35	36	38
51	4	3	3	3	4	4	6	7	8	9	10	12	13	15	16	17	19	20	21	23	24	25	27	28	29	31	32	33	35	36
52	4	3	3	3	3	4	5	6	7	8	10	11	12	14	15	17	18	19	20	22	23	24	25	27	28	29	31	32	33	34
53	4	3	3	3	3	3	4	5	7	8	9	10	12	13	14	16	17	18	19	20	22	23	24	26	27	28	29	30	31	32
54	4	3	3	2	2	3	4	5	6	7	8	9	11	12	13	15	16	17	18	19	20	21	23	24	25	26	27	28	29	30
55	5	4	3	3	2	2	3	4	5	6	7	9	10	11	12	14	15	16	17	18	19	20	21	22	24	25	26	27	28	28
56	6	5	4	3	3	2	3	3	4	5	6	8	9	10	11	13	14	15	16	17	18	19	20	22	23	24	25	25	26	27
57	7	6	5	4	3	3	2	3	3	4	5	7	8	9	10	12	13	14	15	16	18	19	20	21	22	23	23	24	25	25
58	8	7	6	5	4	3	3	3	3	4	5	6	7	8	9	11	12	13	14	16	17	18	19	20	21	22	22	23	24	24
59	9	8	7	6	5	4	4	3	3	3	4	5	6	7	9	10	11	12	13	15	16	17	18	19	20	21	21	22	22	23
60	10	9	8	7	6	5	5	4	4	3	3	4	5	7	8	9	10	11	12	14	15	16	17	18	19	20	20	21	21	21
61	11	11	10	9	7	6	6	5	5	4	3	4	4	5	7	8	9	10	11	13	14	15	16	17	18	19	20	20	20	20
62	13	12	11	10	9	7 M	10	W 7	5	5	4	3	4	5	6	7	8	9	10	11	13	14	15	16	17	18	19	19	19	19
63	14	13	13	12	11	10	9	8	7	6	5	4	3	4	5	6	7	8	9	10	12	13	14	15	16	17	18	18	18	18
64	16	15	14	13	12	11	11	10	9	7	6	5	4	4	4	5	6	7	8	9	10	12	13	14	15	16	17	17	18	18
65	17	18	16	15	14	13	12	12	11	10	8	7	6	5	5	4	5	6	7	8	9	10	12	13	15	16	17	17	17	17
66	18	18	17	16	16	15	14	13	13	11	11	10	9	7	6	5	5	6	7	7	8	9	11	12	15	16	17	17	17	17
67	20	19	19	18	17	17	16	15	14	13	12	12	10	9	8	8	7	6	6	6	7	8	9	11	15	16	17	18	18	18
68	22	21	21	20	19	19	18	17	16	15	14	13	12	11	10	10	9	8	7	7	7	7	7	7	H A	16	19	20	19	18
69	24	23	23	22	21	20	20	19	18	17	16	15	14	13	12	12	11	10	9	9	8	8	8	8	15	17	W A	18	20	19
70	27	26	25	24	23	22	22	21	20	19	18	17	16	15	15	14	13	12	11	10	10	10	10	10	11	12	16	I	22	21
71	29	28	27	26	25	25	24	23	22	21	20	19	18	17	17	15	15	14	13	12	12	11	12	12	13	14	16	21	I	22
72	31	30	29	28	28	27	26	25	24	23	22	21	20	20	19	18	17	16	15	14	13	13	13	14	14	15	17	19	19	20
73	34	33	32	31	30	29	29	28	27	26	24	23	22	22	21	20	19	18	16	16	15	15	15	15	16	17	18	19	20	21
74	36	35	34	33	32	31	31	30	29	27	26	25	23	25 J	27 I	22	20	19	18	17	17	16	16	16	17	17	18	19	20	21
75	38	37	36	35	34	33	33	31	30	29	28	26	25	25	24	23	22	20	19	18	18	17	17	17	18	18	19	20	21	22
76	40	39	38	37	36	35	34	33	32	30	29	28	27	26	25	24	23	21	20	20	19	18	18	18	18	19	20	21	22	23
77	42	41	40	39	38	37	35	35	33	32	31	29	28	27	28	25	24	22	21	20	20	19	19	19	19	20	21	22	22	23
78	43	43	42	41	40	39	38	36	35	33	32	31	30	28	27	26	25	23	22	21	21	20	20	20	20	21	21	22	23	24
79	45	44	43	42	41	40	39	38	36	35	33	32	31	30	28	27	26	24	23	22	21	21	21	21	21	21	22	23	23	24

Table 6B M$_2$ tidal phases δ (°) of the north-central Pacific Ocean.

W / N	177	178	179	180	181	182	183	184	185	186	187	188	189	190	191	192	193	194	195	196	197	198	199	200	201	202	203	204	205	206
30	101	101	101	101	101	102	103	105	105	109	114	123	134	147	162	174	182	172					A	L	A	S	K	A		
31	102	102	102	101	101	101	101	101	101	101	102	107	113	125	136	149	164	168	152	157	162	167								
32	103	103	102	101	100	100	99	99	98	97	97	98	106	106	118	120	141	163	186	214	241	259	250	342	345					
33	104	103	102	101	100	99	98	97	96	95	93	91	89	103	106	107	113	122	139	164	207	304	366	360	344		L A		318	
34	104	103	101	100	99	98	97	95	94	92	89	86	84	81	82	82	85	91	103	117	120	231	292	305		S U	119	315	311	306
35	104	103	101	99	98	97	95	94	92	90	87	83	80	78	76	77	79	82	87	96	104		N	P E	N I	322	317	313	305	306
36	103	102	100	99	96	95	93	92	91	89	86	81	75	71	68	69	70	78	76	A L	A S	K A	337	330	324	321	317	313	305	306
37	103	101	99	97	94	92	91	91	89	89	91	73	61	55	48	U	T I	A N	S	353	342	321	328	325	322	318	315	311	308	304
38	102	103	99	96	92	88	85	83	81	L	E	26	22	16	5	354	356	345	341	342	337	331	327	323	319	316	312	309	308	303
39	80	68	68	65	67	69	70	A	28	10	11	7	4	0	355	349	345	341	338	335	331	327	323	320	316	313	310	307	304	301
40	81	74	67	61	54	46	37	25	19	13	8	3	359	354	350	346	341	337	334	331	327	323	319	316	313	310	307	304	301	299
41	91	73	65	57	49	40	31	23	15	9	3	358	353	349	345	341	337	333	330	326	323	320	317	313	310	307	305	302	299	297
42	81	72	63	53	44	34	26	18	11	4	358	353	348	344	340	336	333	329	326	323	320	317	314	311	308	305	302	300	297	295
43	80	73	60	49	39	29	20	12	5	359	353	348	344	340	336	332	329	326	323	320	317	314	311	308	305	303	300	298	296	293
44	80	69	59	46	35	25	15	7	360	354	349	344	340	336	333	329	326	323	320	317	314	311	309	306	303	301	298	296	294	292
45	80	64	56	43	31	20	10	2	355	349	344	340	336	332	329	326	323	320	317	314	312	309	306	304	301	299	297	295	292	290
46	81	69	54	40	27	15	5	357	350	345	340	336	332	329	326	323	320	318	315	312	310	307	305	302	300	298	296	294	291	289
47	83	69	54	37	23	10	1	353	347	342	337	333	330	326	323	321	318	315	312	310	308	305	303	301	299	297	295	293	291	289
48	85	73	52	34	18	6	357	349	344	339	334	331	327	324	321	319	316	314	311	309	306	304	302	300	298	296	294	292	290	288
49	87	71	50	30	13	2	353	346	341	336	332	329	325	323	320	317	315	312	310	308	305	303	301	299	297	295	293	291	290	288
50	90	73	50	29	11	359	350	344	338	334	330	327	324	321	318	316	313	311	309	307	305	302	300	298	296	294	293	291	289	288
51	95	77	54	29	11	356	348	342	336	332	328	325	322	320	317	315	312	310	308	306	304	302	300	298	296	294	293	291	289	288
52	100	83	59	34	13	353	349	341	335	331	327	324	321	318	316	314	312	310	308	306	304	302	300	298	296	295	293	291	289	288
53	109	97	69	44	19	2	351	342	336	331	326	323	321	318	316	314	312	310	308	306	304	302	300	299	297	295	294	292	290	289
54	116	103	85	59	33	10	355	345	337	331	327	324	321	319	317	315	313	311	308	306	305	303	301	300	299	297	295	293	291	290
55	117	109	96	79	52	25	5	351	340	333	328	325	322	320	318	316	314	312	309	307	306	304	302	301	300	298	296	295	293	291
56	118	113	102	91	74	58	23	2	346	337	330	327	324	322	320	317	315	313	310	309	307	305	304	302	301	299	298	296	295	293
57	118	116	109	109	90	74	49	20	357	343	335	330	326	324	321	319	316	314	311	310	308	307	305	304	302	301	299	298	297	295
58	118	116	113	107	99	88	70	44	15	354	342	335	330	326	323	320	317	315	313	311	309	308	307	306	304	303	302	300	299	298
59	118	117	114	109	102	93	79	62	37	13	355	342	335	330	326	322	319	317	314	312	311	310	309	308	307	306	304	303	302	301
60	119	117	115	112	106	98	86	73	57	36	12	354	342	335	330	325	322	319	316	314	313	312	311	310	309	309	308	307	305	304
61	120	118	117	115	111	101	87	79	70	57	35	10	352	341	334	329	325	322	319	317	316	315	314	314	313	312	311	310	309	308
62	120	119	118	117	115	112	87	85	79	72	58	33	9	352	341	335	330	326	323	321	319	318	318	317	316	316	315	314	313	313
63	120	120	119	118	117	116	114	103	94	85	75	57	33	10	354	344	337	332	328	325	323	322	322	321	320	320	319	319	318	318
64	120	120	119	118	117	116	113	109	104	97	88	75	59	39	10	2	350	341	335	331	329	327	325	325	325	325	325	325	324	324
65	119	119	119	119	118	116	114	111	109	105	98	91	83	72	55	33	13	359	349	341	336	332	330	330	330	330	331	331	331	332
66	118	118	118	118	118	117	115	112	110	106	102	98	93	87	77	65	46	26	10	358	349	341	336	334	334	336	337	338	339	340
67	118	118	118	118	118	116	115	113	110	107	104	100	96	91	84	76	67	53	38	22	9	350	348	340	338	342	343	345	347	348
68	118	118	118	118	117	116	115	113	111	108	106	102	98	94	88	82	75	69	60	49	38	23	10	349		356	348	351	355	357
69	118	118	118	118	118	117	116	114	112	110	107	103	99	95	91	87	82	77	70	63	54	45	37	29	47	23		11	4	5
70	119	119	119	119	118	117	116	115	113	111	108	104	101	96	93	89	86	82	77	71	65	59	54	52	53	46	62		6	12
71	120	120	120	119	119	118	117	115	114	112	109	107	103	98	95	91	88	86	82	77	72	66	61	58	56	53	53	55		31
72	121	121	121	120	120	119	118	117	115	113	112	109	105	100	96	94	91	89	85	81	76	71	66	61	58	54	54	52	47	38
73	122	122	122	122	121	121	120	119	117	116	114	110	106	99	95	95	93	91	88	84	80	74	70	68	61	57	55	52	47	42
74	122	122	122	122	122	121	121	120	119	117	115	113	110	108	105	98	96	94	91	87	83	78	73	69	64	60	56	53	49	45
75	123	123	123	123	123	122	122	121	119	118	117	115	113	111	107	103	100	97	93	89	85	81	76	72	67	62	58	55	51	48
76	124	124	124	124	124	123	123	122	121	119	118	117	115	113	110	107	103	100	96	92	87	83	78	73	69	64	66	56	53	50
77	125	125	125	125	125	124	124	123	122	121	120	118	116	114	112	109	106	103	99	94	89	84	79	75	78	65	61	58	54	51
78	126	126	126	126	126	126	125	125	124	123	121	120	118	116	114	112	109	108	102	97	92	86	81	76	71	67	63	59	56	53
79	127	127	127	127	127	127	127	126	125	124	123	122	120	118	116	114	112	109	104	99	94	88	83	78	73	69	65	61	58	54

Table 7A M_2 tidal amplitudes ξ (cm) of the central Pacific Ocean.

	162	163	164	165	166	167	168	169	170	171	172	173	174	175	176
71	22	23	24	25	26	29	29	30	30	30	30	30	30	30	30
72	23	24	25	27	28	29	30	31	32	32	32	33	33	32	32
73	24	26	27	28	30	31	32	33	34	34	35	35	35	35	34
74	25	27	29	30	31	33	34	35	36	36	37	37	37	37	37
75	27	28	30	32	33	34	36	37	38	38	39	39	39	39	39
76	28	30	32	33	35	36	38	39	39	40	41	41	41	41	41
77	30	32	33	35	37	38	40	41	41	42	42	43	43	43	42
78	31	34	35	37	39	41	42	43	43	44	44	44	44	44	44
79	32	36	37	38	44	45	50	45	46	46	46	46	46	46	46
80	34	37	38	40	42	45	46	48	47	48	48	48	47	47	47
81	36	38	39	40	42	44	47	47	48	48	49	49	49	48	48
82	37	38	40	42	43	44	47	47	48	49	51	50	50	50	49
83	37	39	41	42	43	44	45	49	48	49	50	51	51	51	50
84	38	40	42	43	44	45	45	46	50	50	52	52	52	52	51
85	39	41	42	44	45	46	44	46	47	50	51	53	53	53	52
86	40	42	44	45	46	47	48	48	49	50	50	52	53	54	53
87	41	43	45	46	47	48	49	50	50	51	51	52	55	55	54
88	43	44	46	47	48	49	50	51	52	53	53	55	57	56	55
89	43	45	46	48	48	49	50	51	53	53	54	57	58	58	56
90	44	45	47	48	49	50	51	52	54	54	55	56	57	58	57
91	44	46	47	48	50	51	51	52	50	54	55	55	58	58	59
92	45	46	48	49	50	51	52	53	51	54	55	55	54	59	52
93	45	46	48	49	50	51	52	53	53	54	54	54	54	53	57
94	45	46	47	49	49	50	51	52	53	54	54	54	54	54	53
95	44	45	47	48	48	50	50	51	52	53	54	54	54	54	54
96	44	45	46	46	47	48	49	50	51	52	53	53	54	54	54
97	43	44	45	45	46	47	49	49	50	51	52	53	54	54	54
98	43	43	43	43	44	46	47	48	50	51	52	53	53	54	54
99	40	39	40	41	42	44	46	48	49	51	52	53	53	54	54
100	SOLO-	33	36	37	39	42	45	47	49	50	51	52	53	54	54
101	MONS	29	32	34	37	41	43	46	48	50	51	52	53	54	54
102	21	26	28	31	33	36	41	45	47	49	51	52	53	53	54
103	17	22	26	29	31	34	40	44	46	48	50	51	52	53	53
104	15	19	23	26	29	33	38	45	47	48	49	51	52	53	53
105	14	17	21	24	27	32	39	45	47	48	49	51	52	53	54
106	14	17	20	23	26	30		44	45	48	49	50	52	53	54
107	16	18	21	24	26	35		45	49	48	49	50	51	53	54
108	19	20	23	26	28	29	34		43	47	47	49	53	52	54
109	22	23	28	29	30	31	32	36	40	44	46	46	49	50	52
110	27	27		34	33	33	34	36	38	43	46	47	48	50	51
111	32	33	34		32	35	35	36	37	43	45	47	48	49	50
112	38	37	38	52		37	36	38	39	41	44	46	47	48	49
113	41	40	40	40	41	[illegible]	38	39	41	42	44	46	47	48	49
114	44	43	42	41	40	44	38	39	42	44	45	46	48	49	50
115	46	45	44	43	42	41	40	41	43	44	46	47	49	50	50
116	49	47	46	45	44	43	42	43	44	45	47	48	50	50	51
117	51	49	48	47	46	45	45	45	46	47	48	50	51	52	52
118	53	51	50	49	48	48	48	48	48	49	50	51	53	53	54
119	54	53	52	51	50	51	52	52	52	52	52	53	55	55	55
120	56	55	53	53	52	52	57	55	55	55	55	56	57	57	57

	177	178	179	180	181	182	183	184	185	186	187	188	189	190	191
71	29	28	27	26	25	25	24	23	22	21	20	19	18	17	17
72	31	30	29	28	28	27	26	25	24	23	22	21	20	20	19
73	34	33	32	31	30	29	28	28	27	26	24	23	22	22	21
74	36	35	34	33	32	31	31	30	29	27	26	25	23	25	27
75	38	37	36	35	34	33	33	31	30	29	28	26	25	25	24
76	40	39	38	37	36	35	34	33	32	30	29	28	27	26	25
77	42	41	40	39	38	37	36	35	33	32	31	29	28	27	26
78	43	43	42	41	40	39	38	36	35	33	32	31	30	28	27
79	45	44	43	42	41	40	39	38	36	35	33	32	31	30	28
80	46	45	45	43	42	41	40	39	38	36	35	33	32	31	29
81	48	47	46	45	44	43	41	40	39	37	36	35	33	32	30
82	49	48	47	46	45	44	42	41	40	39	37	36	34	33	31
83	50	49	48	48	46	45	44	42	41	39	38	37	35	34	32
84	51	50	50	49	48	46	45	43	42	40	39	38	36	34	33
85	52	51	51	50	49	47	46	44	43	41	40	38	37	35	33
86	53	52	52	51	49	48	47	45	44	42	41	39	37	36	34
87	54	53	52	51	50	49	48	46	45	43	41	40	38	36	35
88	55	54	53	52	51	49	48	47	45	44	42	40	39	37	35
89	55	56	53	52	51	50	49	47	46	44	43	41	39	37	35
90	55	56	53	52	51	50	49	47	46	44	43	41	40	38	36
91	55	56	53	52	52	50	49	48	46	45	43	42	40	38	36
92	55	56	53	53	52	50	49	48	47	45	43	42	40	38	36
93	56	54	53	53	51	50	49	48	47	45	44	42	42	38	36
94	51	54	53	53	52	50	49	48	47	45	43	42	39	37	35
95	54	54	53	53	52	50	49	48	47	45	43	43	39	37	35
96	54	54	54	53	52	50	49	48	46	45	43	40	39	37	35
97	54	54	54	53	52	50	49	48	46	45	43	41	39	37	35
98	54	54	53	53	51	50	49	48	46	45	43	41	39	37	35
99	54	55	52	56	51	50	49	48	47	45	43	41	39	37	35
100	54	53	52	51	51	50	50	48	47	45	43	41	39	37	35
101	54	54	53	52	52	51	50	49	47	45	43	41	39	36	34
102	54	55	54	53	53	51	50	49	47	45	43	41	39	36	34
103	54	49	55	54	52	52	51	50	47	45	43	42	36	36	34
104	53	57	56	55	54	52	51	53	46	44	43	41	38	36	35
105	54	56	56	55	53	52	50	47	46	44	42	38	37	37	33
106	55	57	55	54	52	51	49	47	45	44	41	38	37	36	33
107	55	55		[illegible]	51	49	48	46	45	43	39	38	37	36	34
108	61			52	47	48	47	46	45	43	39	38	38	37	35
109	52	59	55	51	48	49	48	46	46	44	40	40	38	33	35
110	51	49	49	49	49	49	48	47	46	51	38	39	38	37	32
111	50	50	50	50	50	49	48	47	46	50	39	39	39	38	36
112	50	50	51	51	50	49	47	46	52	46	40	40	39	39	38
113	50	51	51	51	50	49	47	45	41	41	41	41	40	39	39
114	51	51	52	52	51	49	47	45	43	42	42	42	41	40	39
115	51	52	52	52	52	50	48	45	44	43	43	42	42	41	40
116	52	52	53	53	52	50	48	46	45	44	44	43	42	42	41
117	53	53	53	53	52	50	48	46	46	45	44	44	43	42	41
118	54	54	54	53	52	50	48	47	45	46	45	44	43	43	42
119	55	55	54	53	51	50	48	47	47	46	45	45	44	43	42
120	56	56	55	53	51	50	49	48	47	46	46	45	44	43	42

Table 7B M_2 tidal phases δ (°) of the central Pacific Ocean.

λ \ φ	162	163	164	165	166	167	168	169	170	171	172	173	174	175	176	177	178	179	180	181	182	183	184	185	186	187	188	189	190	191
71	120	119	119	119	119	115	121	120	120	120	119	119	119	120	120	120	120	120	119	119	118	117	115	114	112	109	107	103	98	95
72	119	118	118	119	120	121	122	120	120	120	120	120	120	121	121	121	121	121	120	120	119	118	117	115	113	112	109	105	100	96
73	118	119	118	119	119	120	120	120	120	120	120	121	121	121	122	122	122	122	122	121	121	120	119	117	116	114	110	106	95	95
74	118	118	118	118	119	119	119	119	119	120	120	121	121	122	122	122	122	122	122	122	121	121	120	119	117	115	113	110	106	105
75	117	117	118	118	118	118	119	119	119	120	120	121	122	122	123	123	123	123	123	123	122	122	121	119	118	117	115	113	111	107
76	117	117	118	118	118	118	118	119	120	120	121	122	122	123	123	124	124	124	124	124	123	123	122	121	119	118	117	115	113	110
77	117	118	118	118	117	117	118	119	120	121	122	123	123	124	124	125	125	125	125	125	124	124	123	122	121	120	118	116	114	112
78	118	118	119	118	117	116	117	119	121	122	123	124	124	125	126	126	126	126	126	126	126	125	125	124	123	121	120	118	116	114
79	118	120	121	119	120	124	124	121	122	122	124	125	125	126	127	127	127	127	127	127	127	127	126	125	124	123	122	120	118	116
80	122	126	123	122	122	123	123	125	124	124	125	126	127	127	128	128	129	129	129	129	128	128	127	127	126	125	124	122	121	119
81	125	125	124	123	123	127	125	126	125	125	126	127	128	128	129	129	130	130	130	130	129	129	129	128	128	127	126	124	123	121
82	125	125	125	125	126	126	127	127	128	128	126	128	129	130	130	130	131	131	131	131	131	130	130	129	129	129	128	127	125	124
83	126	127	127	127	128	128	128	123	128	127	128	130	130	131	131	132	132	132	133	132	132	132	132	131	131	130	130	129	128	126
84	128	129	128	129	130	130	130	130	127	129	130	131	132	133	133	133	134	134	134	134	134	134	133	133	133	132	132	131	130	128
85	129	129	132	132	132	132	132	132	123	132	131	133	134	134	135	135	135	135	136	136	135	135	135	135	134	134	133	132	131	130
86	131	132	133	133	133	133	134	134	135	135	135	132	136	136	136	136	137	137	137	137	137	137	137	136	136	135	134	134	133	131
87	133	133	134	135	135	135	136	136	137	137	136	132	138	138	138	138	138	139	139	139	139	139	139	138	137	137	136	135	134	133
88	135	135	136	137	137	137	138	138	138	139	139	139	140	140	140	140	140	140	141	141	141	141	140	140	139	138	138	137	136	135
89	137	138	138	139	139	139	139	140	140	141	141	146	149	142	142	142	142	142	142	143	143	143	142	142	141	140	139	139	138	136
90	139	140	140	140	141	141	141	142	143	143	144	145	152	144	144	144	144	144	144	144	144	144	144	143	143	142	141	140	139	138
91	141	142	142	142	143	143	143	144	149	146	145	146	148	145	145	145	145	146	146	146	146	146	146	145	145	144	143	142	141	140
92	143	143	144	144	144	145	145	146	148	148	147	147	147	144	143	147	147	148	148	148	148	148	148	147	147	146	145	144	143	142
93	145	145	146	146	146	147	147	148	149	149	149	149	150	150	150	149	149	149	149	150	150	149	149	149	145	149	148	145	144	144
94	147	147	148	148	148	149	150	150	151	151	151	151	152	152	152	152	151	151	151	151	151	151	151	151	152	152	148	148	147	147
95	149	150	150	150	151	151	152	153	153	153	153	154	154	154	154	153	153	153	153	153	153	153	153	153	154	154	152	151	150	150
96	151	151	151	152	152	153	154	155	156	156	156	156	156	156	156	156	155	155	154	155	155	155	155	155	155	155	155	154	154	153
97	154	153	153	153	154	155	156	157	158	158	159	159	159	159	158	158	157	156	156	156	156	157	157	157	157	157	157	157	157	157
98	156	155	154	155	156	157	158	159	160	161	161	161	161	161	161	160	159	158	157	157	158	158	159	159	159	159	159	159	160	160
99	154	156	156	157	159	160	161	162	163	163	164	164	163	163	163	162	162	161	153	158	160	160	161	161	161	161	162	162	163	163
100	SOLO-	149	159	160	162	163	164	165	165	166	166	166	166	165	165	165	164	163	162	161	162	162	163	163	164	164	164	165	165	167
101	MONS	152	163	162	158	159	160	168	168	169	168	168	168	168	167	167	166	166	165	164	164	165	165	165	166	166	167	167	168	170
102	153	164	165	165	164	163	173	172	172	172	171	171	171	171	171	171	170	169	168	168	167	167	167	168	169	169	168	169	171	173
103	175	173	171	171	169	168	170	176	176	176	175	175	174	174	175	175	173	172	171	171	171	170	169	170	172	173	168	171	172	176
104	189	182	180	177	175	175	176	186	180	180	179	179	178	178	178	178	174	174	174	173	173	174	178	172	175	178	173	172	176	179
105	205	195	198	185	184	184	179	183	183	183-	183	182	182	181	181	180	179	176	175	175	176	176	176	176	177	186	183	186	175	183
106	219	207	199	194	191	187		185	187	186	186	186	185	185	184	182	179	177	175	177	178	179	180	180	181	182	185	188	187	189
107	231	210	207	200	197	196	NEW HEBRIDES	189	191	190	190	189	189	189	188	186	195	J	S	181	182	183	184	185	186	187	188	190	191	192
108	242	220	214	205	202	201	197		197	194	194	194	193	193	193	195	F	I	195	189	187	188	189	189	190	190	191	192	193	194
109	252	242	210	200	205	204	204	200	199	198	198	199	198	198	198	198	196	197	200	196	193	192	193	194	195	192	194	197	203	196
110	260	255		210	209	208	208	209	209	205	204	204	204	203	203	203	204	204	203	201	195	196	197	197	191	195	197	195	203	204
111	269	269	268		216	212	212	213	213	211	210	209	209	208	207	207	207	207	206	204	202	200	199	197	191	197	199	201	204	206
112	280	276	275	275		221	218	217	218	217	215	214	213	212	211	211	210	210	209	207	205	203	203	[illegible]	200	208	202	203	205	206
113	284	279	276	275	270		236	225	223	222	220	219	217	216	215	214	213	212	212	210	208	206	208	203	204	204	204	205	206	207
114	285	281	277	274	270	267	244	234	229	226	224	222	221	219	217	216	216	215	214	213	211	209	207	206	206	206	206	206	207	208
115	287	282	277	273	269	264	254	242	235	231	228	225	223	221	220	219	218	217	216	215	213	211	208	207	207	207	207	208	208	209
116	289	283	278	273	269	265	257	248	240	235	231	228	226	224	222	221	220	219	218	217	215	213	209	208	208	208	208	209	209	210
117	290	284	279	274	271	266	266	252	245	239	235	231	228	226	224	222	221	220	219	217	215	213	210	209	209	209	209	209	210	210
118	290	284	280	276	272	268	262	255	249	244	239	234	231	228	226	224	222	221	220	218	216	213	210	210	210	209	209	210	210	210
119	290	285	281	277	274	270	264	258	252	248	243	238	233	230	227	225	223	221	220	217	215	211	210	210	210	209	209	210	210	210
120	291	287	283	279	276	273	264	260	255	251	246	240	234	231	229	225	223	221	219	217	214	210	209	209	209	209	209	209	210	210

In the area of Tables 4A and 4B, a major amphidromic point is visible in the Caribbean Sea southeast of the island of Puerto Rico (PRI) near the marked deep-sea gauge station. The loosely connected Caribbean and Atlantic tides rotate counterclockwise around this point with the 0° = 360° cotidal line running northeastward. As a result of this rotation, the whole Caribbean Sea appears to be trapped and unable to develop any significant M_2-tide. In agreement with the observations, the M_2 tidal crest sweeps across the Caribbean Sea essentially from north to south with very little variation in water level.

If one follows the tidal crest around the amphidromic point from the Atlantic Ocean to the Caribbean Sea and back to the Atlantic, one recognizes a major tidal distortion caused by ocean ridges, which has long been discovered by practical tidalists (see, e.g., Harris, 1904 I; Bogdanov, 1961 I; Defant, 1961 I; and Luther and Wunsch, 1974 I). As the tide crosses the ridge between the islands, it suffers a distinct amplitude jump and a significant phase shift. For example, north of Puerto Rico (PRI) and Hispaniola and in the southeast around Barbados (BB), the computed and empirical Atlantic tide data display a higher water level and an earlier or, respectively, a delayed cresting time than the adjacent tide data on the Caribbean side. In particular, in full agreement with the observations, the tidal retardation time can easily exceed 30° (~1 hour). The distortion seems to depend on the angle with which the tidal crest spills over the ridge. Maximum distortion appears to be associated with a normal crossing. It may be pointed out that the realistic resolution of tidal distortions by ocean ridges (see below) constitutes probably the most significant improvement of the new model over all earlier hydrodynamical models.

The Atlantic portion of the Caribbean–Atlantic amphidromic rotation is opposed by a southward advancing tide from about Newfoundland in the north and by an eastward progressing tide from about Cape Cod to Cape Hatteras in the west. As a result of this interaction of three opposing tidal waves, the middle latitudes (around n = 60°) of the Atlantic display very small variations in tidal amplitudes and phases. In the high-amplitude sections between Nova Scotia and Cape Cod and between Cape Hatteras and Florida's coast, the Caribbean–Atlantic rotation wave seems to be less affected by the opposing tidal waves and progresses frontally against the corresponding shallow coastal corners.

Since the tide-generating M_2-potential is a single progressing wave from east to west, the ocean responds with amphidromic tidal waves that cannot reverse their directions. Thus, at shore points tidal waves are either incoming or outgoing without reversals. In the first case tidal crests always move from sea to shore. In the second case tides always swell to their crests at the shore first and then move out to sea. The incoming tide between Nova Scotia and Cape Cod seems to produce high and rough waters. The outgoing tide between Cape Cod and Cape Hatteras is distinctly lower.

Although the computed tide in the Gulf of St. Lawrence displays the well-known amphidromic point (Defant, 1961 I), the grid system is much too crude to attach a high accuracy to the tidal constants in this border sea. For the same reason, the tidal data listed between Florida, Cuba, and the Bahamas are naturally less accurate than those in the open oceans.

Tables 5A and 5B illustrate the smoothness with which the computed tide of the northeastern Pacific Ocean attaches itself to the empirical tide data along the North American west coast. The tidal constants observed at the islands of Guadalupe (GI) and Farallon (FI), at the Cobb Seamount (CS), and at the included nearshore deep-sea stations fit realistically well into the computed surrounding tide. The amplitudes and phases of the excluded offshore deep-sea measurements in the Pacific agree within 2 cm and 6°, respectively, with the computed data (Table 3), which is just the same accuracy as in the Atlantic.

Perhaps the most prominent feature of this area is the amphidromic point ⍟, around which the M_2-tide rotates counterclockwise. This amphidromic system was predicted by Munk *et al.* (1970) and Irish *et al.* (1971) in almost identical geographical position. Earlier hydrodynamical tide models failed to resolve this system on proper location, although several models matched the empirical data along the coast quite well. Since the northeastern

Pacific falls short in major bottom and coastal irregularities when compared to the northwestern Atlantic, the indicated rapid loss of quality in westerly direction seemed disappointing. Yet, as will be demonstrated below, this shortcoming could have been concluded from the obvious failure of those models to reasonably reproduce the tide over most of the north and central Pacific Ocean.

As was mentioned before, the author's preliminary tide model (Schwiderski, 1976 I) used a bathymetry that failed to represent the hydrodynamical barrier effects of the Marianas, Nampo, Kuril, Aleutian, and Hawaiian ridges, as well as of other seamount chains. Consequently, the M_2-tide of almost the whole central, western, and northern Pacific area was modeled as a single huge amphidromic system, as pictured by the similar maps of other numerical tidalists such as Zahel (1971 I) and Estes (1975 I, 1977 I). The clockwise-rotating Pacific tide was free to sweep undisturbed into the Philippine, Okhotsk, and Bering seas. By the time the computed tidal crest reached the Aleutian Islands, it was just about 180° out of phase. When the original bathymetry was replaced by hydrodynamically defined depth data (section, "Hydrodynamically Defined Ocean Bathymetry"), the entire Pacific Ocean resembled a whirlpool after some continued computations over several quarter periods. The amphidromic system weakened, and its center slipped slowly southward, but drastically improved phases appeared gradually along the Aleutian Ridge, confirming the anticipated effect of ocean ridges.

The complete turnaround of the Pacific M_2 tide near the Aleutian Islands was speeded up when the empirical tidal constants were introduced into the model. In fact, a repeat of the same computations settled the Pacific Ocean tide into its final position in a rather dramatic fashion. Striking improvements were registered over the whole Pacific and, of course, also over the Atlantic and Indian oceans.

As is depicted in Tables 6A and 6B for the north-central Pacific, the amphidromic system is replaced by a low-amplitude tide. It appears to be locked in between the Aleutian and Hawaiian ridges in the north and south and also between the Emperor Seamount chain in the west and the high-amplitude tide in the east, which progresses in a westerly direction from the west coast of North America (Tables 5A and 5B). The amplitude topography of this area resembles the low-amplitude tide in the Caribbean Sea (Table 4A). When the westward-advancing tidal wave enters the region between the Aleutian and Hawaiian ridges, it suffers a remarkable, almost symmetric retardation at both ridges. In fact, as the visible ($0° = 360°$) cotidal line in Table 6B reveals, the crest front of the tidal wave assumes the shape of an almost symmetric wedge. If one traces the 0° phase line westward beginning at both ridges, one can infer a definite idea about the realistic reproduction of the tide in this region. At both ends, the 0° phase is in full agreement with the empirical data. As the observed phases grow westward along both ridges, so grow proportionally the distances of the 0° phase line from the ridges.

The new computed M_2-tide model no longer indicates any symptoms of the original phase problems at the Aleutian and Hawaiian ridges. The computed amplitudes and phases approach the empirical tidal constants from both sides of the ridges as smoothly as could be desired. As the tidal wave spills over both ridges in northwestward or southwestward directions, respectively, it suffers a tidal distortion similar to that found before at the Caribbean Ridge. Amplitude jumps and major phase shifts are again in complete agreement with observations (see the remarks of Luther and Wunsch, 1974 I). It is particularly gratifying to find the phase shift well developed along the whole length of the Hawaiian Ridge from the island of Hawaii to Midway, even though only few stations of data were used at both ends. Also, it may be noticed that the observed tidal constants at the distant and isolated island stations of Pribilof (PF), Midway (MW), and Johnston (JI) are all realistically well integrated by the surrounding computed tide.

Ironically, the old and new M_2-tide maps constructed by Bogdanov (1961 I) and Luther and Wunsch (1974 I) by pure intuition and simple rules of thumb from empirical data came closest to the present charts. Indeed, their maps display no amphidromic system in the north-central Pacific. As is verified in Schwiderski

(1979c I), the computed amphidromic points between the Cook and Society islands and near the southern edge of the Solomon Islands are both in almost identical positions with those charted by the same authors. Nevertheless, their detailed distribution of amplitudes and phases is still significantly different from the present one.

Perhaps the most spectacular display of the high quality of both the computed and the observed tidal data is brought out by Tables 7A and 7B depicting the high-amplitude tide of the central Pacific. Indeed, unlike any other open ocean area, the tabulated region is dotted with numerous tide-gauge stations at island groups and at scattered isolated islands. In addition to the fully listed island chains, there are the isolated islands: Johnston (JI), Wake (WI), Kudaie (KI), Ocean (OI), Funafuti (FI), Wallis (WI), Niue (NI), and Norfolk (NF). The corresponding observed tidal constants listed in nongeographical arrangement appeared incoherent and, hence, uncorrelated, giving rise to doubt their true value. Yet, the computed tidal wave sweeps across the whole area in a southwesterly direction with little variation of its high amplitude. As the wave crest passes through the many checkpoints with correct height and in right time, it integrates and correlates without a single exception all the empirical data into one coherent unity.

Conclusions

The quality evaluation of the constructed M_2 ocean tide model described in Parts I and II of this paper leads to the conclusion that it is now possible to compute detailed and accurate global ocean tides which fulfill the application requirements of contemporary researchers. In fact, it is estimated that the computed M_2-tide charts permit an M_2-tide prediction anywhere in the open oceans with an accuracy of better than 5 cm. This accuracy leaves ample room for superposable errors due to the additional smaller tidal constituents listed in Table 1 of Part I, which are presently under construction with equivalent relative accuracy. When all those partial tides become available, the total tide-prediction error is expected to fall well below the 10-cm limit needed in many applications.

Naturally, the achieved high accuracy of the M_2-tide in the open oceans drops somewhat near continental or island stations where empirical data are missing or are less accurate themselves (see the introduction to the British Admiralty Tide Tables, 1977 I). This is particularly true near Antarctica and in the Arctic Ocean, where reliable measurements of ocean tides and depths are sparse. Also, less accurate predictions must be anticipated in small border seas, bays, estuaries, and channels where the 1° by 1° grid system precludes a sufficient resolution. To improve the present tide model in those areas, significantly improved observations will be needed along with a locally refined network and corresponding bathymetric data.

Acknowledgments

It is the author's most pleasant obligation to acknowledge the sustained and generous sponsorship by Mr. Ralph A. Niemann, Head, Strategic Systems Department, Mr. R. J. Anderle, Head of the Astronautics and Geodesy Division, and his Associate, Dr. C. Oesterwinter, who followed the slowly progressing work with patience and confidence. In the current two years this project is supported by the NAVSWC Independent Research Fund and by a grant from the National Geodetic Survey/NOS/NOAA. The author wishes to thank his colleagues, Dr. C. J. Cohen and Dr. B. Zondek, for many critical and stimulating discussions and suggestions. Special acknowledgment must be extended to the author's programmer, Mr. L. Szeto, for his competent and effective preparation of all the involved computer programs and his untiring cooperation in carrying out seemingly unending program changes, many of which could not be mentioned in this treatise.

Excerpts of this paper were presented at the International Symposium on Interaction of Marine Geodesy and Ocean Dynamics, held from Oct. 10 to 13, 1978, at the Rosenstiel School of Marine and Atmospheric Science, Miami, Florida 33149.

References

Cartwright, D. E., 1971, Tides and Waves in the Vicinity of St. Helena. Phil. Trans. Roy. Soc., London, Ser. A, 270, p. 603.

Gallagher, B. S., Shimada, K. M., Gonzales, F. L., Jr., and Stroup, E. D., 1971, Tides and Currents in Fanning Atoll Lagoon. Pacific Sci., 25, p. 191.

International Hydrographic Bureau, 1966, Tides, Harmonic Constants. Spec. Publ., No. 26, Monaco.

Irish, J., Munk, W. H., and Snodgrass, R., 1971, M_2 Amphidrome in the Northeast Pacific. Geophys. Fluid. Dyn., 2, p. 355.

Munk, W. H., Snodgrass, F., and Wimbush, M., 1970, Tides Offshore: Transition from California Coastal to Deep-Sea Waters. Geophys. Fluid. Dyn., 1, p. 161.

National Ocean Survey, 1942, Tidal Harmonic Constants. U.S. Coast and Geodetic Survey, Washington, D.C.

Schwiderski, E. W., 1979, Ocean Tides, Part I: Global Ocean Tidal Equations. Marine Geodesy, Vol. 3.

Zetler, B., Munk, W., Mofjeld, H., Brown, W., and Dormer, F., 1975, MODE Tides. J. Phys. Oceanogr., 5, p. 430.